CONTACT METAMORPHISM OF METAPELITES IN

THE FRONT RANGE, COLORADO: A STUDY

OF DISEQUILIBRIUM REACTIONS

by

Donald Eugene Cameron
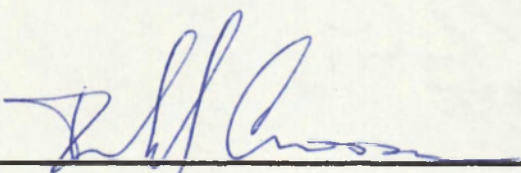

———————————————————

A Thesis Submitted to the Faculty of the

DEPARTMENT OF GEOSCIENCES

In Partial Fulfillment of the Requirements
For the Degree of

MASTER OF SCIENCE

In the Graduate College

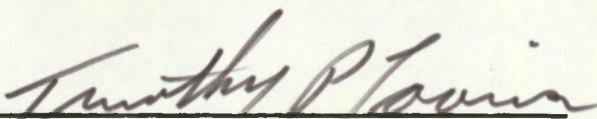THE UNIVERSITY OF ARIZONA

1 9 7 6

STATEMENT BY AUTHOR
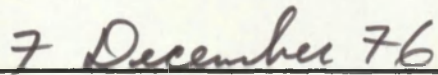
APPROVAL BY THESIS DIRECTOR

This thesis has been approved on the date shown below:

_____   _7 December 76_
TIMOTHY P. LOOMIS   Date
Associate Professor of Geology

ACKNOWLEDGMENTS

TABLE OF CONTENTS

TABLE OF CONTENTS—Continued

LIST OF TABLES

LIST OF ILLUSTRATIONS

ABSTRACT

Contact metamorphism of Precambrian upper amphibolite facies grade metapelites by a Laramide stock near Nederland, Colorado produced pseudomorph and other reaction textures reflecting the disequilibrium present in samples collected. The initial regional assemblage is quartz-sillimanite-biotite-cordierite-garnet-K-feldspar-plagioclase-magnetite.

The breakdown of garnet to cordierite, magnetite, and quartz was studied in detail from polished section. Garnet is zoned with respect to Fe^{2+}, Mg, and Mn to constant edge composition, and Ti-poor green biotite (cf. brown regional) forms inside "atoll" garnets. The data suggest reactions such as:

$$1.0 \text{ Garnet(core)} + .47 \text{ K-feldspar} + \nu_{H_2O} H_2O \rightarrow .51 \text{ Garnet(rim)} +$$
$$.07 \text{ Cordierite} + .53 \text{ Biotite(green)} + .06 \text{ Anorthite(component}$$
$$\text{in plagioclase)} + .93 \text{ Quartz} \tag{4a}$$

and,

$$.51 \text{ Garnet(rim)} + .16 \text{ Biotite(green)} + .20 \text{ O}_2 \rightarrow .27 \text{ Cordierite}$$
$$+ .12 \text{ Quartz} + .05 \text{ Anorthite} + .14 \text{ K-feldspar} + .40 \text{ Magnetite}$$
$$+ \nu_{H_2O} H_2O. \tag{4b}$$
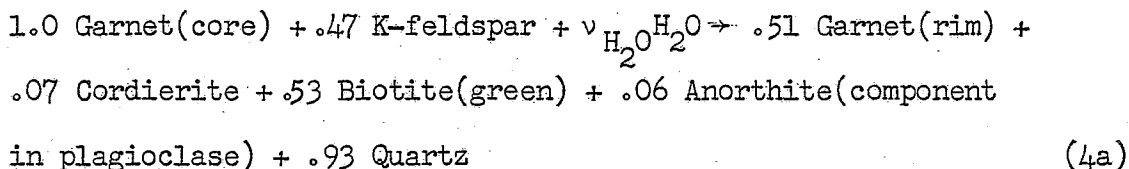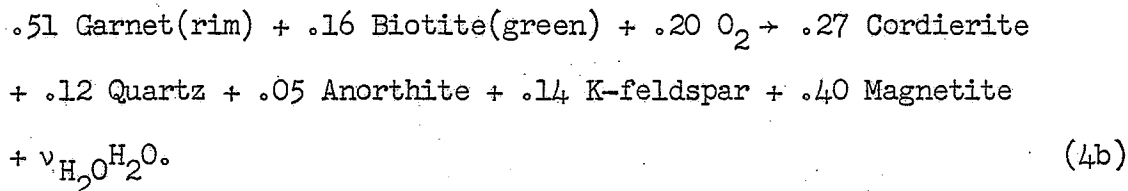
To produce product green biotite (reaction 4a) K_2O and H_2O must diffuse into the pseudomorph from the matrix because K-feldspar was

not originally in garnet. If Al_2O_3 remained relatively immobile,
CaO and SiO_2 diffused outward and inward, respectively. Reaction 4b
is slower. Intermediate product, green biotite, is partially
consumed (reaction 4b).

Closer to the contact and with increasing oxidation sillimanite
and biotite break down according to the reaction:

3 Fe-Mg-Biotite + 6 Sillimanite + 6 Quartz + $\frac{1}{2}$ O_2 → 3 Fe-Mg-
Cordierite + 3 K-feldspar + 1 Magnetite + 3 H_2O,
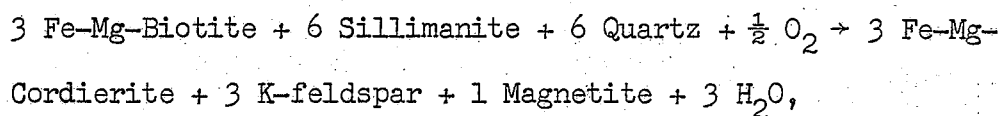
based on textural evidence.

INTRODUCTION

Two of the major goals of the study of metamorphic rocks are:
1) deducing their conditions of formation, and 2) deducing the sequence
of events involved in the mineralogical and textural evolution of a
sample, and thereby, of larger rock units. Few "regionally" metamor-
phosed rocks show unequivocal evidence of the manner in which the
reactions necessary to attain, or maintain, equilibrium were accom-
plished. The textural and mineralogical evolution of certain regional
metamorphic rocks has been interpreted in the recent literature with
regard to reaction mechanisms and processes of ion transport (Rast
1965, Mueller 1967, Carmichael 1969, McAteer 1976, Misch and
Onyeagocha 1976) where gradients in the intensive variables in the
sample were small. In these cases, the initial configuration of the
rock was known to some extent with regard to the distribution of
chemical components and mineral phases; however, in the case of the
Whetstone Lake pelites (Carmichael 1969), some of the reactions which
are assumed to have taken place cannot be demonstrated texturally. If
unique interpretations of textures are not possible, the conclusions
reached concerning reaction mechanisms and textural evolution are
affected by assumptions made about the conditions and processes in-
volved in mineral reactions and component migration, and thus are
ambiguous.

1

Disequilibrium amongst mineral phases provides information in deciphering reaction processes and is therefore of great interest. As examples, compositional zoning profiles in garnet have been applied to problems of partial melting and crystallization at depth (Fitton 1972), tectonics related to metamorphism (Griffin 1971a, 1972; Griffin and Råheim 1973; Griffin and Heier 1973; Loomis 1975; Råheim 1975), and mineral growth and reaction (Harte and Henley 1966; Hollister 1966, 1969, 1970; Bryhni and Griffin 1971; Griffin 1971a, 1972; Chinner 1962; Okrusch 1971; Grant and Weiblen 1971; Edmunds and Atherton 1971; Kurat and Scharbert 1972; Misch and Onyeagocha 1976). Spatial zonation of mineral assemblages in volumes of rock has long been a subject of interest in studies of metasomatism, and, more recently, of strongly overstepped reactions. Examples of interest are articles by Vidale 1969; Griffin 1971b, 1972; Griffin and Råheim 1973; and Loomis 1976a, -b.

The collection of some of this type of data has come before an adequate understanding of the choice of controlling processes was available; and yet consideration of the process involved in metamorphism of a small amount of sample can be very instructive in formulating a model for the overall reaction. If the overall reaction is the sum of two or more steps, e.g., dissolution of a mineral, and diffusion of ions to a nucleating or growing product mineral, one of the steps must limit the reaction rate at any given time or under a given set of imposed conditions. Experimentalists recognize the importance of surface energy effects when in some cases they seed an experimental charge; but when, for example, reversals are difficult to

obtain, an explanation is not usually obvious. In a successful experiment, all evidence of the rate-controlling process is obliterated. Because diffusion can generate readily apparent textures such as mineral zonation during a run, it is often assumed to have controlled the textural development and mineral compositions.

The relative importance of dissolution-precipitation or diffusion in a given reaction has still not been given sufficient attention; e.g., garnet zoning profiles indicate a need for measuring certain diffusion constants to test the consequences of multicomponent diffusion in that mineral. In recent years, much attention has been drawn to the local equilibrium, or intergranular diffusion experiments, and theoretical modelling of natural processes has followed observation of intramineral and mineral assemblage zonation in natural rocks (cf. Thompson 1959, Vidale 1969, Fisher 1973, and others).

An obvious environment from which to collect data pertinent to kinetic problems of all kinds is a contact metamorphic aureole, because gradients in the intensive variables are steep and are of relatively short duration. In addition, the P, T boundary conditions are usually better known than for most metamorphic rocks. Careful consideration of textures and compositional data can be used to outline the equilibrium assemblage and in some cases can serve as constraints on the possible chemical reactions involved.

An ideal area is the Front Range Mineral Belt, Colorado, because Tertiary stocks have affected metapelites formed during a previous episode of metamorphism. Detailed sampling of Precambrian

gneisses in the contact aureole of the Caribou stock, Nederland, Colorado, was undertaken to study the reaction processes involved in reconstitution of the regional metamorphic mineral assemblage to one reflecting the contact metamorphism. Large changes in the intensive variables — pressure, temperature, and the fugacities of components in the vapor phase — resulted in compositional shifts in minerals involved in chemical reactions. Reactions involved the breakdown of regional garnet, sillimanite, and biotite to cordierite-bearing assemblages. The textural relations of reactant and product minerals as seen in thin section, and detailed electron microprobe analysis of phase compositions can be used to quantitatively model the chemical reactions and to outline the equilibrium assemblages.

Geologic Setting

The Caribou stock is one of a series of shallow Laramide intrusives which crop out west of Boulder, Colorado, in the central Front Range of the Rocky Mountains (fig. 1). The intrusions lie along the northeastern extension of the Colorado Mineral Belt and were the site of intensive mining activity around the turn of the century. In the vicinity of Nederland, the stocks passively intrude Precambrian gneisses of the Idaho Springs Formation and are generally steep-sided bodies that crosscut pre-existing structures and foliation in the gneisses. The Caribou stock ranges in composition from diorite to quartz monzonite and is possibly a composite intrusion.

The crystalline rocks intruded by the Caribou stock include quartz-microcline gneiss, hornblende-plagioclase gneiss, and
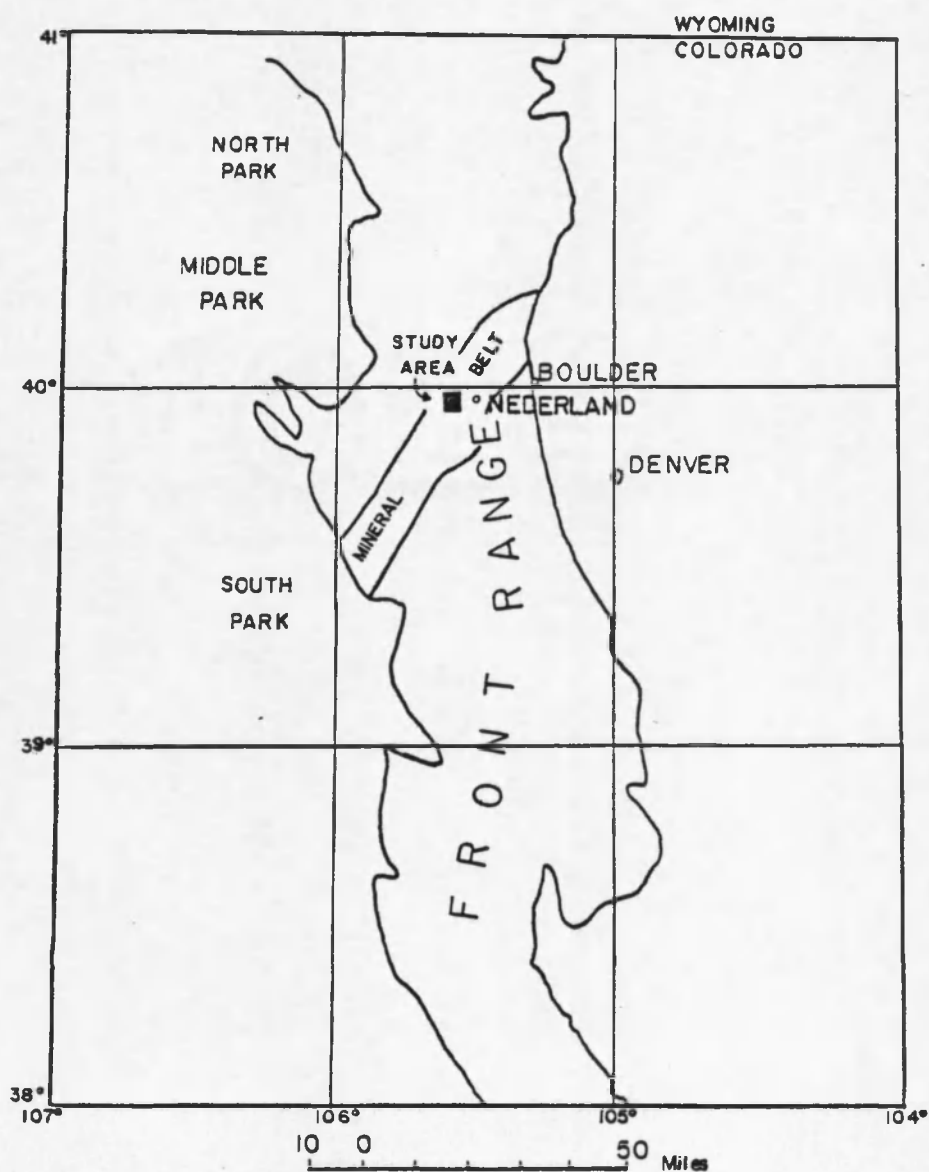
Figure 1. Map of Front Range, Colorado, showing area of study and outline of the mineral belt. — (After Lovering and Goddard 1950).

metapelite of the Idaho Springs Formation, as well as younger, batholithic, Precambrian Boulder Creek Granodiorite. The gneisses are above the sillimanite-K-feldspar isograd as defined by Evans and Guidotti (1966). The thermal imprint of the stock on the gneisses is most pronounced in the metapelites, which have been recrystallized as much as one-half mile from the contact, and in which hydrothermal activity was most intensely concentrated. Care was taken to avoid sampling altered rocks. The outcrop relations of the various units are depicted in figure 2.

Previous Work

The most recent mapping of the Caribou stock and adjacent gneisses was accomplished by Gable and Sims (Gable, Sims, and Weiblen 1970; cf. Smith 1938, Lovering and Goddard 1950). The area was included in a regional mapping and chemical study of pelitic rocks in the Idaho Springs Formation by the same authors (Gable and Sims 1969).

Steiger and Hart (1967) and Wright (1967) discussed the petrography and mineralogical aspects of the microcline-orthoclase transition within the aureole of the Eldora (or Bryan Mountain) stock two miles to the south. The former authors also computed heat-flow models of the probable temperature distribution about that stock. Shieh and Taylor (1969) determined O^{18}/O^{16} and D/H ratios for rocks and selected minerals in the Eldora and Caribou stocks and contact aureoles. They interpret the O^{18}/O^{16} whole-rock data to preclude any lateral exchange of material between the plutons and contact aureoles except over a distance of several feet at the contact. Isotopic
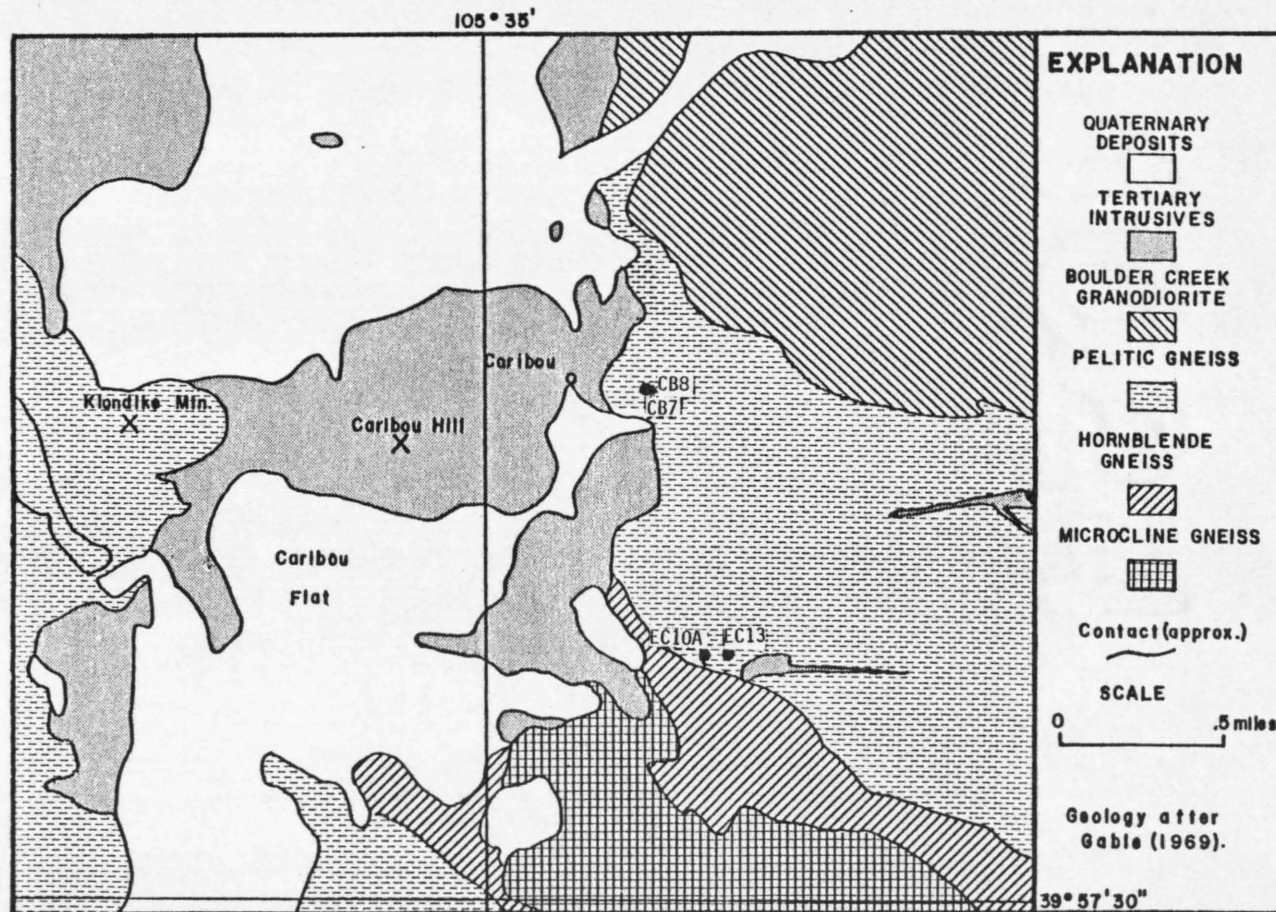
Figure 2. Generalized map of bedrock geology in the vicinity of the Caribou stock showing sample locations.

mineral temperatures were calculated from quartz-magnetite and quartz-biotite pairs, the former being more internally consistent, and in better accord with their heat-flow model.

Gable et al. (1970) made a study of selected samples from the Tertiary aureoles including two samples from the contact aureole of the Caribou stock. A general description of the contact effects, petrographic data, and a discussion of the conditions of metamorphism deduced from the metamorphic reactions and the heat-flow model of Steiger and Hart (1967) were outlined. Their paper provided a basis for the detailed study presented here, and some of their results are discussed and summarized in this paper (Appendix I).

Sampling

Thin sections (44) were cut from samples collected along traverses approximately perpendicular to the stock contacts. Five samples were chosen as representative and used for reconnaissance microprobe study; of these, two samples, EC13 and CB7, were selected for detailed study. The locations of the hand specimens discussed in this paper are shown in figure 2. Table I lists the mineral assemblages of the chosen samples arranged by degree of alteration. A complete sample location map and a discussion of the geology and petrography of the contact and regional gneisses are included in Appendix I.

Table I. Mineral assemblages present in selected
           samples from the Caribou aureole.

Mineral	EC13	EC10a	CB7	CB11a
Quartz	X	X	X	X
K-feldspar	X	X	X	X
Biotite	X	X	X	X
Andalusite				X
Kyanite		X		
Sillimanite	X	X	X	X
Hercynite				
Ilmenite			X	X
Magnetite	X	X	X	X
Garnet	X	X	X	X
Cordierite	X		X	X
Oligoclase	X	X	X	X
Muscovite	X		X	X

ANALYSIS AND INTERPRETATION OF
REGIONAL GARNET BREAKDOWN

Description of Regional Assemblage

The regionally metamorphosed assemblage that was studied comprises quartz-sillimanite ($\pm$ kyanite)-biotite-magnetite-ilmenite-K-feldspar-plagioclase $\pm$ garnet $\pm$ cordierite gneiss (EC10a in table I), and is preserved without significant evidence of reaction in some of the more quartzose rocks in the aureole. All of the above minerals can apparently be found in a single thin section.

Hercynite is sporadic in occurrence and was found in one thin section in the contact aureole containing all of the above minerals except regional cordierite. Cordierite may rim garnet or is present as anhedral porphyroblasts in the matrix (Gable and Sims 1969, p. 19, Gable et al. 1970, p. 671); no texturally obvious relict (regional) cordierite was found in any thin sections from the Caribou aureole. Rounded or flattened garnets are variously encased in quartz and plagioclase, or between foliae of biotite and sillimanite.

The photomicrograph in figure 3 illustrates some of the textural characteristics of a relatively unaffected outer aureole rock (EC10a). The garnet contains small inclusions of quartz and biotite and numerous throughgoing cracks which contain quartz, green biotite and magnetite considered part of the contact alteration assemblage. Sillimanite needles are included in garnets in other thin sections.
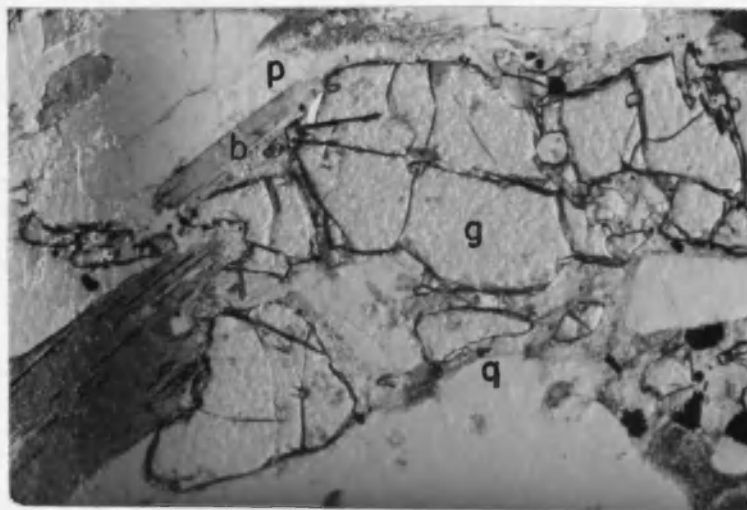
Figure 3.   Photomicrograph of polished thin section EC10a. — Garnet
(g) is in a matrix of quartz (q), plagioclase (p), and
brown biotite (bb). Plane-polarized light. Note quartz
inclusions in garnet and alteration along cracks at right
side of photo. 65X.

Description of Outer Aureole
Contact Assemblage

Textural evidence of reactions involving the breakdown of regional garnet to cordierite-bearing contact assemblages is found in what is here called the outer aureole. Garnet is largely reacted in sample EC13, giving rise to pseudomorphs of cordierite, along with some biotite, magnetite, and quartz. The sample is no closer to the contact than is EC10a, the representative regional rock. The pseudomorph textures were described by Gable et al. (1970), but a more detailed description is presented here.

The photomicrographs presented in figure 4 are of several domains displaying reaction in a single polished thin section. The pseudomorphs preserve the outline of the original garnet and lie in a matrix of sillimanite, biotite (brown), and quartz. Some anhedral plagioclase grains may be found nearby. Well-formed prisms of sillimanite and large brown biotite grains are ragged where they project into the pseudomorph. Minor muscovite is present along the rims of the pseudomorphs intergrown with (replacing?) biotite or sillimanite. In another thin section from a nearby outcrop (EC17), a green spinel (hercynite?) was found near the pseudomorph as anhedral grains within biotite; there is no textural evidence of it having been involved directly in the reaction as a reactant or product. Anhedral K-feldspar associated with an incipient breakdown of biotite or as porphyroblasts in quartz is present; magnetite grains are strung out along cleavages in the biotite.
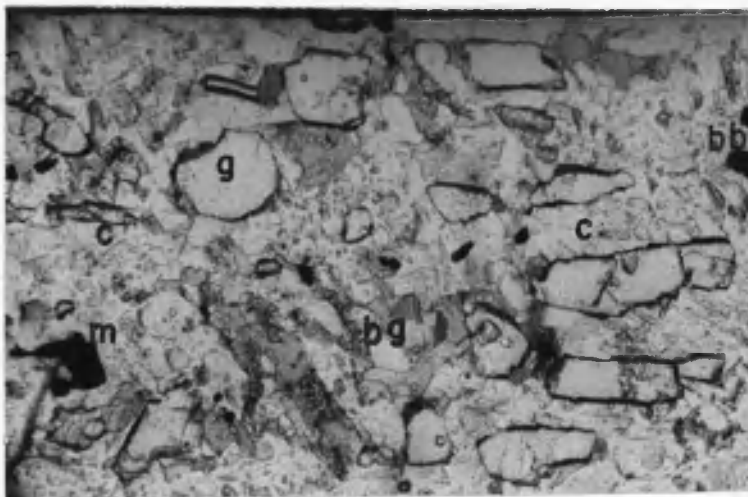
(a) Cordierite pseudomorph after garnet (c, cordierite; bg, green
biotite; s, sillimanite; m, magnetite). Small specks are green
biotite in cordierite.
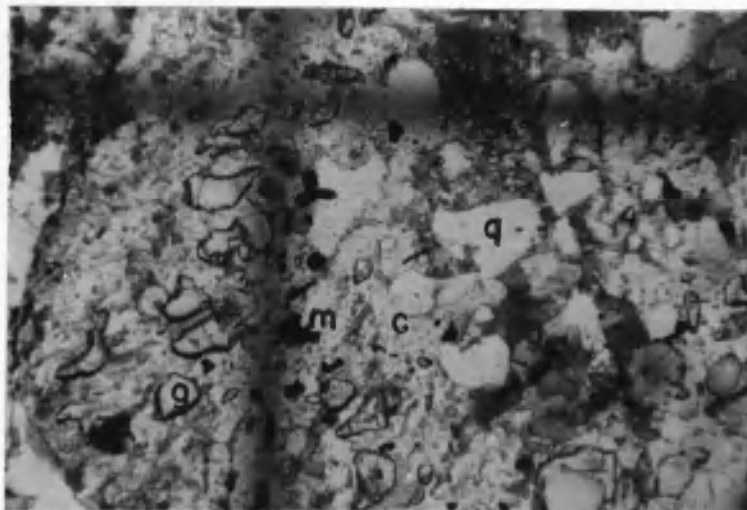
(b) "Atoll" structure of garnet from another pseudomorph.

Figure 4. Photomicrographs of polished thin section EC13. — Plane-
polarized light. Orthogonal lines are location grid. 65X.
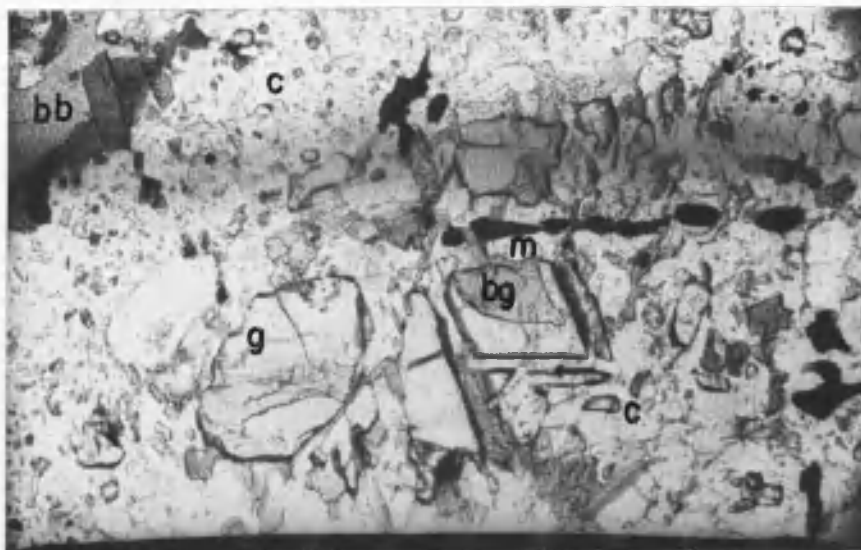
(c) Interior of large pseudomorph showing development of cordierite, magnetite, and green biotite in garnet cracks. Portion of outer rind is at left.
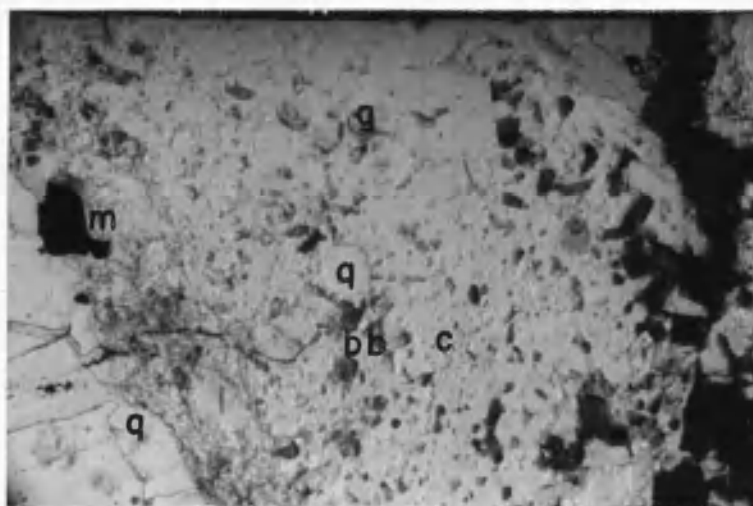
(d) Small pseudomorph with remnants of garnet only below the surface of the section.

Figure 4, continued.
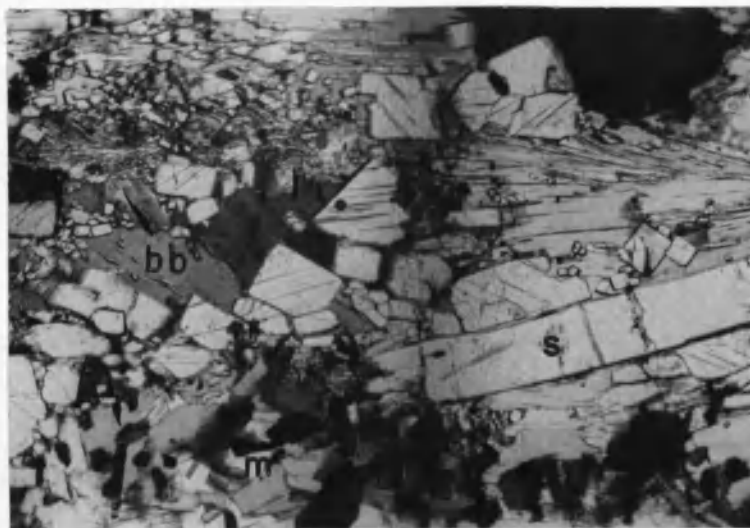
(e) Matrix of sillimanite and brown biotite.

Figure 4, continued.

The variation in modal abundance and distribution of product phases within the pseudomorphs is marked, as can be seen from comparison of figures 4a, b, c, and d. An outer rind of cordierite, with specks of green, or greenish-brown biotite and sparse magnetite, is usually present and contains almost no garnet remnants. This rind is thickest where the surrounding minerals are sillimanite and biotite. The inner "core" of the pseudomorphs is richer in green biotite, and large, rounded quartz grains are often present. Cordierite may be a very minor constituent of the inner zone (core), but in pseudomorphs of lesser size in which the garnet has almost completely disappeared (fig. 4d), cordierite is present in about the same amount as in the outer rind throughout.

Garnet remnants (50 to 200μ diameter) are most abundant just inside the outer rind and near the core of the pseudomorph, giving rise to "atoll" textures (cf. Rast 1965, p. 95). Where garnet grains are in abundance they form a mosaic of straight, matching edges (figs. 4a and 4c) because breakdown occurred along pre-existing cracks. Magnetite in euhedral crystals intergrown submicroscopically(?) with quartz forms in the core of the cracks flanked by biotite, and this relict texture is still preserved where the process has advanced as in EC13. Magnetite is only rarely in contact with garnet; the rounded quartz grains in, e.g., figure 4a, may have been present prior to reaction.

Muscovite is present with K-feldspar, sillimanite (or sporadic andalusite), and quartz in the polished sections studied in detail

from the outer and inner aureoles. Large, tabular crystals seem to replace the latter minerals, or are growing in quartz next to either sillimanite or biotite. The euhedral character and size of these muscovite crystals distinguish them from the fine-grained sericite that is observed in many thin sections, and which appears to represent "later" alteration. However, abundant K-feldspar in association with biotite breakdown textures suggests that K-feldspar and sillimanite were compatible; therefore, the textures do not allow a solution to the problem of whether K-feldspar or muscovite, or both, are stable.

The matrix in EC13 has no texture interpreted as reaction of biotite and sillimanite to form cordierite, and apparently represents an oriented fabric preserved from the Precambrian metamorphism (fig. 4e).

The textural observations made above suggest an overall reaction for the breakdown of garnet as follows:

$$\text{Fe-Mg-Garnet} + \text{Fe-Mg-Biotite} + \text{Quartz} + O_2 \rightarrow \text{Fe-Mg-Cordierite}$$
$$+ \text{Magnetite} + \text{Anorthite} + \text{K-feldspar} + H_2O, \tag{1}$$
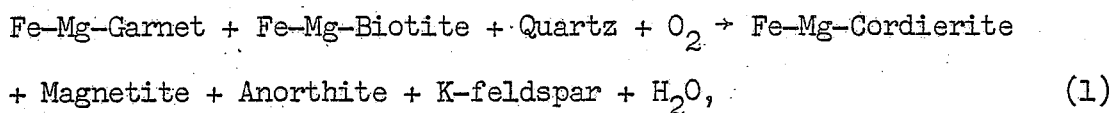
which is similar to that formulated by Gable et al. (1970, p. 679).

Nature of the System to be Analyzed

While the overall reaction 1 documents the changes taking place in the sample during contact metamorphism, it is the goal of this study to combine petrographic and compositional data to discern a possible mechanism for the reaction in terms of the mobility of chemical components. It is evident from previous work in the field that

interpretation of chemical and textural data and the kinetics of reactions requires definition of the system and of the scale at which it is observed.

One system of interest is the volume of rock represented by the scale of the thin sections. The reactions themselves, however, may be taking place on a much smaller scale which could be deciphered from textures or from mass balance calculations (Carmichael 1969, Loomis 1976a, Misch and Onyeagocha 1976). The domain considered is the smallest volume which contains the reactant and product minerals, and may include an intergranular fluid. In this study, the domain in which reaction is taking place is texturally represented by the pseudomorph minerals, and perhaps minerals in the immediate surroundings.

Several of the pseudomorphs in a single polished thin section were studied in detail. The presence of compositional zoning in the garnet remnants, color variation between biotites in different surroundings, and the complicated and variable paragenesis within the pseudomorphs require study in order to determine at what volume scale equilibrium was achieved.

Analysis of Data

Display of Microprobe Data

Selected major element analyses of garnet, cordierite, and biotite are listed in table II, and most of the data for one domain are projected from K-feldspar and quartz in the AFM diagram, figure 5.

Table II. Selected major element analyses of garnet, cordierite, and biotite. — The analyses were performed on ARL-EMX microprobes at the University of Wisconsin and University of California, Los Angeles, using an accelerating potential of 15KV and .015uamp sample current measured on brass. The minimum beam diameter was used, being 1-2μ for rim compositions. Data were corrected using correction factors (Bence and Albee 1968). Garnet analyses were re-run using the ZAF correction program developed by Tracor Northern, Inc. Insignificant differences in values for FeO and MgO resulted from this procedure. Spots analyzed were checked for internal consistency at each laboratory.

Sample*	1	2	3	4	5	6	7	8
Lab No.	UWG11	UWG15	UCLAJ	UCG2N	UCG1A	UCG4A	UCG1W	UW
SiO_2	36.60	36.48	47.74	34.99	34.49	34.64	35.84	50.63
Al_2O_3	21.66	20.40	32.08	18.62	21.06	19.80	18.43	32.72
MgO	5.85	1.55	6.15	6.57	7.76	6.55	7.87	7.22
FeO_t	32.00	34.40	11.45	22.95	25.40	22.99	21.39	10.22
MnO	.93	5.55	.48	.20	.16	.20		.25
TiO_2			0.0	2.82	.09	2.42	3.48	0.0
CaO	1.60	1.38	.12	.19	.18	.08	0.0	.01
Na_2O			.09	.23	.29	.26	.19	.08
K_2O			.05	8.97	8.48	9.15	9.31	0.0
H_2O**	0.0	0.0	1.81	4.40	2.06	3.87	3.45	0.0
Total	98.64	99.77	99.97	99.94	99.97	99.96	99.96	101.13
X_{Mg}/X_{Fe}	.32	.08	.95	.51	.54	.49	.66	1.26

*1 — (EC13) Garnet core composition (fig. 4).
 2 — (EC13) Garnet rim composition (same grain as above).
 3 — (EC13) Cordierite next to biotite and magnetite (fig. 4).
 4 — (EC13) Biotite in matrix (brown).
 5 — (EC13) Biotite (green within pseudomorph next to garnet and cordierite.
 6 — (EC13) Biotite (greenish-brown) next to cordierite on edge of pseudomorph.
 7 — (CB7) Biotite next to cordierite.
 8 — (CB7) Cordierite next to biotite (above).
**H_2O computed by difference.
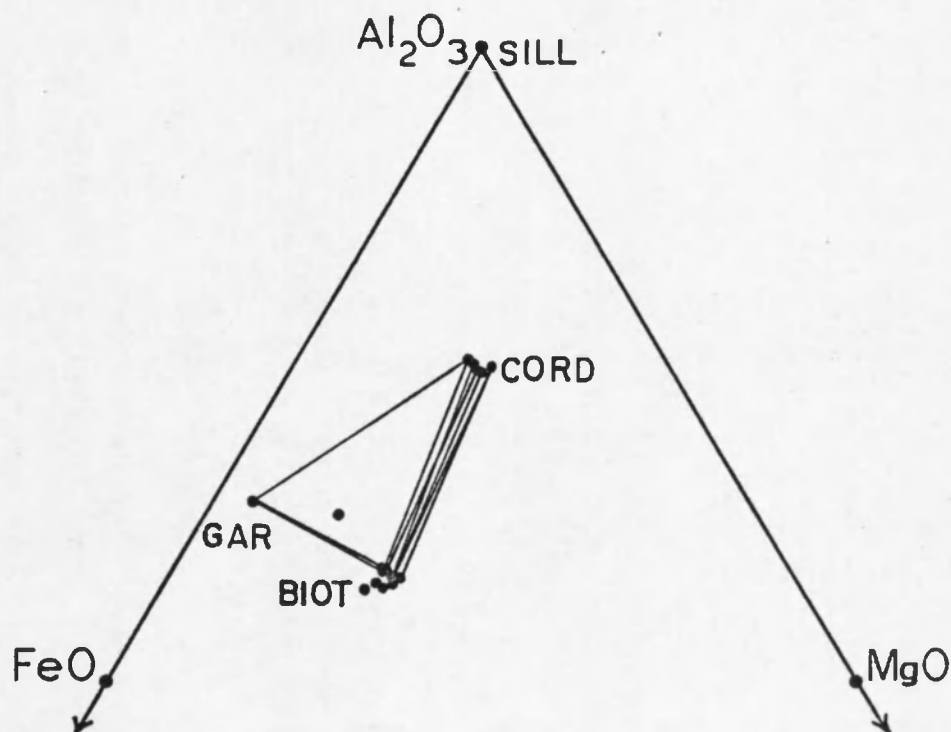
Figure 5. AFM projection from K-feldspar of selected probe analyses
of biotite, cordierite, and garnet in a pseudomorph in
sample EC13. — Tie lines connect grain boundary composi-
tions of coexisting pairs. Rim compositions of the
garnet and phases touching garnet are constant within
analytical error. The less aluminous biotites are inter-
mediate to brown in color.

Tie lines are drawn between coexisting phases as analyzed. The representation suffers because of the number of components needed to fully depict the system, but certain compositional relationships can be shown in the presence of magnetite. Ti^{4+} in biotite, and spessartite and grossularite in garnet, as well as Fe^{3+} in all the phases analyzed are not considered in the projection. On inspection of figure 5 and table II, the following points should be noted: 1) analyses (three) of garnet "cores" (meaning the portions of garnet remnants having constant composition) are rich in pyrope compared to analyses (four) of garnet rims, which have a constant composition; 2) matrix biotites (brown) enclosed in sillimanite or _next_ to the pseudomorph are Al-poor and plot below green biotite (in fig. 5), which is restricted to within the pseudomorph; but, 3) Mg/Fe ratios of green biotite fall in the same range as for matrix biotite.

Compositional Characteristics of Biotite

Because f_{O_2} of the system was within the magnetite field it is reasonable to expect that biotite was partially oxidized (Mueller 1972, p. 310). The color difference between biotites, however, in EC13 may be related to their titania content (table II, analyses 4 and 5) rather than to their oxidation states as had been proposed earlier (Gable et al. 1970, p. 672). Green biotite is always low in Ti and high in Al relative to brown biotite in the thin section. Values for (Ti + Al) using mole fraction data were computed for all the biotites analyzed in a given probe run. A similar correlation between the Ti and Al contents of biotite and its color was obtained by calculation

of (Ti + Al) from the limited data of Chinner (1960, Table 5), Hall (1941), and Misch and Onyeagocha (1976, Table 3). No correlation with (tetrahedral) Si was found; this lack of correlation indicates that the Al^{3+} in octahedral coordination is that affected by the substitution of Ti^{4+}. Wones and Eugster (1965, p. 1257) also recognize $Al^{3+} \rightleftharpoons Ti^{4+}$ substitutions in biotite. The substitutions involving Fe^{3+} and $Ti^{4+} \rightleftharpoons Al^{3+}$ would both affect the H_2O content of biotite. The water contents (computed by difference) for all brown and green biotites are also averaged in table III, but instrument drift and the method of calculating H_2O preclude an accurate determination.

Compositional Characteristics of Garnet

The compositional variation of garnet is evident from step scans (figs. 6a, b, c) on the garnet remnants shown in figure 4a. Mg drops sharply, whereas Fe and Mn climb significantly toward the rim in a zone $\sim 30\mu$ wide. The profiles generated all show two changes in slope, indicating that, e.g., multi-component diffusion cross-coupling or a multi-stage reaction history could be responsible for what is observed. Large non-ideal interaction between Mn and Mg (Ganguly and Kennedy 1974) could affect the shape of the zoning profiles in the case of multicomponent diffusion coupling. Figures 6a-c are profiles of a series of garnet remnants located in the center to near the edge of a pseudomorph, respectively. The garnet core compositions are the same in each grain, and therefore the zoning present probably does not represent, and is not affected by, an original (Precambrian) growth or reaction zoning profile in the garnet.

Table III. Comparison of H_2O and (Ti + Al) for biotites.

	Sample Size	H_2O (wt. %)	(Ti + Al)*
Brown Biotite	8	3.9	1.88
Green Biotite	9	4.5	1.88
$\overline{N}$ =		4.2	1.88
S.D. =			.04

*Reported in formula number based on 12 oxygens.

STEP SCAN - GAR A IN EC13 UCLA PROBE
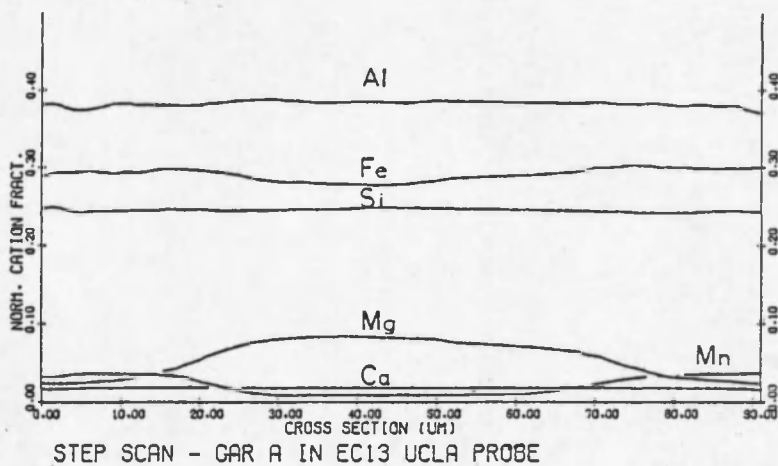
(a) Edge-to-edge step scan on garnet remnant.

STEP SCAN ON GAR B IN EC13.
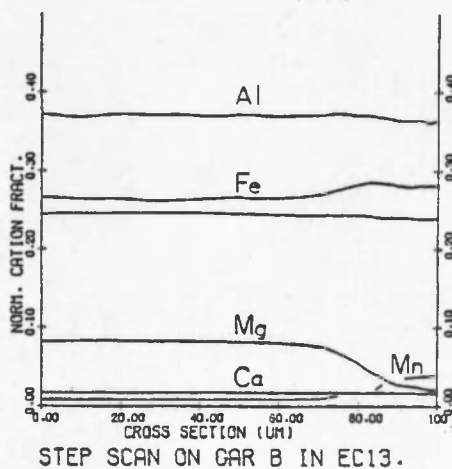
(b) Center-to-edge step scan on garnet remnant.

Figure 6.   Step scans of zoned garnet remnants in a single pseudomorph
            in EC13. — a, b, and c are in order of increasing distance
            from the pseudomorph center. Horizontal scale is distance
            in microns from edge of grain.

STEP SCAN ON GAR D IN EC13.
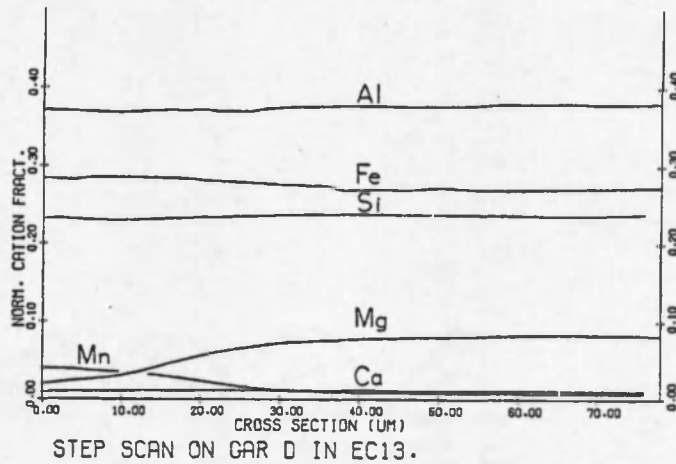
(c) Edge-to-center step scan on garnet remnant.

STEP SCAN ON GARNET IN EC10A
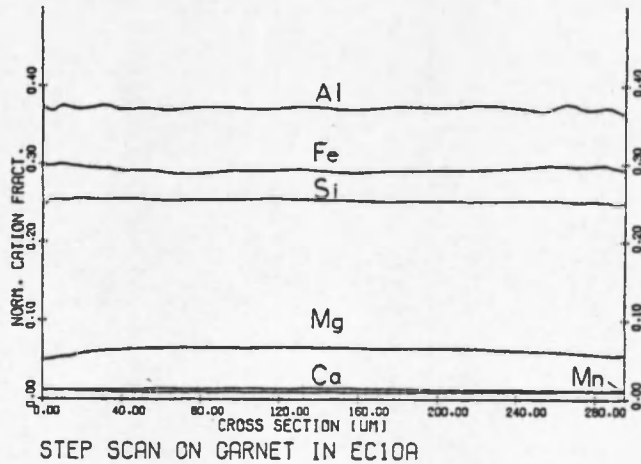
(d) Unzoned garnet in sample EC10a assumed to be characteristic of
     regional garnet.

Figure 6, continued.

Figure 6d is a step scan of a virtually unzoned garnet in the unreacted sample from the aureole (EC10a) shown in figure 3. It would lend support to the hypothesis that there was no primary zoning in regional garnet.

The rim composition of the garnet does not differ in composition from grain to grain, nor does it depend on whether garnet is adjacent to cordierite or biotite, within the precision of the analyses.

Attainment of Equilibrium and the Equilibrium Assemblage

Element partitioning data can be used to evaluate the extent to which equilibrium was attained in the pseudomorph assemblage. Mg–Fe partitioning, in particular, is most useful because that ratio is sensitive to changes in the intensive variables T and f_{O_2}. The slopes of the tie lines between coexisting garnet rim, cordierite, and biotite are related to K_D, the distribution coefficient for Mg/Fe, and are observed to be nearly parallel between different pairs in EC13.

Values of K_D for garnet rim–biotite pairs (fig. 5) were compared with the data of Heitanen (1969) for similar temperatures (discussed below), and show agreement. Assuming that garnet rims have a constant composition and assuming that equilibrium Mg-Fe partitioning with biotite and cordierite are satisfied under the assumed conditions, the rim composition of garnet appears to be stable in the system as far as can be determined from compositional data. These criteria for suggesting the approach to equilibrium have been applied in previous

studies by Edmunds and Atherton (1971) and by Loomis (1975). Other possible evidence of garnet stability is the observation that some garnet is present in every pseudomorph, regardless of size.

No textural evidence of incompatibility of biotite with silli-manite was noted in the same sample, or from others collected nearby. At arbitrary T, P, and f_{O_2}, garnet, cordierite, sillimanite, and biotite should not all coexist with quartz, K-feldspar, magnetite, oligoclase, and a vapor phase (where the system is $SiO_2-Al_2O_3-FeO-MgO-Na_2O-K_2O-H_2O-O_2$) unless, e.g., 1) some component such as MnO or CaO stabilized garnet as a phase, or 2) sillimanite and biotite are incompatible, but the reaction for some reason has not taken place. CaO in garnet is essentially constant in the zoned garnets, but since MnO is higher in garnet rims in the sample, the latter component could presumably have stabilized garnet. The second possibility cannot be verified with the data available.

The minerals present in the outer aureole which may constitute the partial equilibrium (Helgeson 1968) contact assemblage is from the considerations above suggested to be quartz-garnet-cordierite-silli-manite-biotite-magnetite-plagioclase-K-feldspar. Garnet cores are considered to be isolated from the equilibrated minerals by garnet rim.

Comparison of Regional and Outer Aureole Contact Assemblages

Graphical Display of the Assemblages

The contact metamorphism caused measurable compositional shifts in the garnet-bearing assemblage as well as changes in partitioning of

Mg and Fe between garnet, biotite, and cordierite. This can be shown in a limited way by projecting both the regional and contact metamorphic assemblages on a diagram subject to some conditions and assumptions. Both assemblages are assumed to be in equilibrium with plagioclase, magnetite, and quartz. These are considered "excess" components in the sense of Korzhinskii (1959) and are thus used as projection points.

K-feldspar is also used as a projection point notwithstanding its apparent coexistence with muscovite in the outer and inner contact aureole. Estimated temperature and pressure conditions of the aureole (Lovering and Goddard 1950, Gable et al. 1970, this paper, below) may lie within the field of the divariant isograd reaction:

K-Na Muscovite + Quartz + Albite (component in plagioclase)

= K-Na-Orthoclase + Sillimanite + H_2O (2)
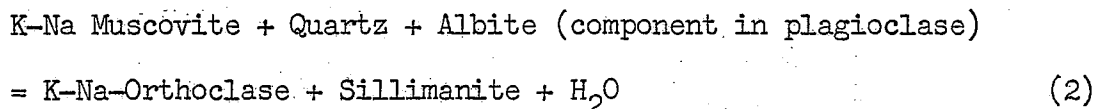
(Evans and Guidotti 1966), whereas the regional gneisses are above the reaction. The compositions of feldspars and muscovite were not studied, but the experimental data and documented temperature range of the reaction in western Maine could explain the observed associations. The choice of K-feldspar instead of muscovite as a projection point is thus somewhat arbitrary, but will not significantly reduce the usefulness of the projection for analysis of the relations between garnet, cordierite, biotite, and sillimanite. Alternatively, the coexistence of sillimanite, K-feldspar, and muscovite may simply reflect the range of temperatures in the aureole during heating and cooling.

The resulting projection, figure 7, is the AFM diagram used widely in simpler pelitic systems. Unfortunately, the regional assemblage is not completely understood and is apparently a disequilibrium one. Cordierite is present with garnet, sillimanite, and biotite in some of the regional assemblages studied by Gable and Sims (1969) and as a relict regional mineral in some of the contact metamorphosed rocks studied by Gable et al. (1970). Thus, the regional topology cannot be safely extrapolated from their data for purposes of thermodynamic analysis of the changes to the contact metamorphic topology. Instead, measured compositions of regional garnet, biotite, and cordierite reported by Gable et al. (1970) and measured from the unreacted sample (EC10a in table I) in this study are shown as phase triangle $\underline{A}$ in figure 7. Reliable partitioning data are not available to indicate whether or not compositions chosen are reasonable for the estimated conditions (630 to 700°C, 3 to 5kb, f_{O_2} in the magnetite field) of regional metamorphism in the Front Range (Gable and Sims 1969). The tie lines have no actual significance here other than to distinguish the regional mineral compositions from those measured from the contact assemblage (triangle $\underline{B}$) containing garnet rim, green biotite and cordierite. Sillimanite and biotite were probably compatible in the regional rocks, and possibly were also compatible in the outer aureole. Figure 7, therefore, will only be used in a qualitative manner to illustrate the compositional shifts and changes in partitioning between the minerals connected by tie lines.
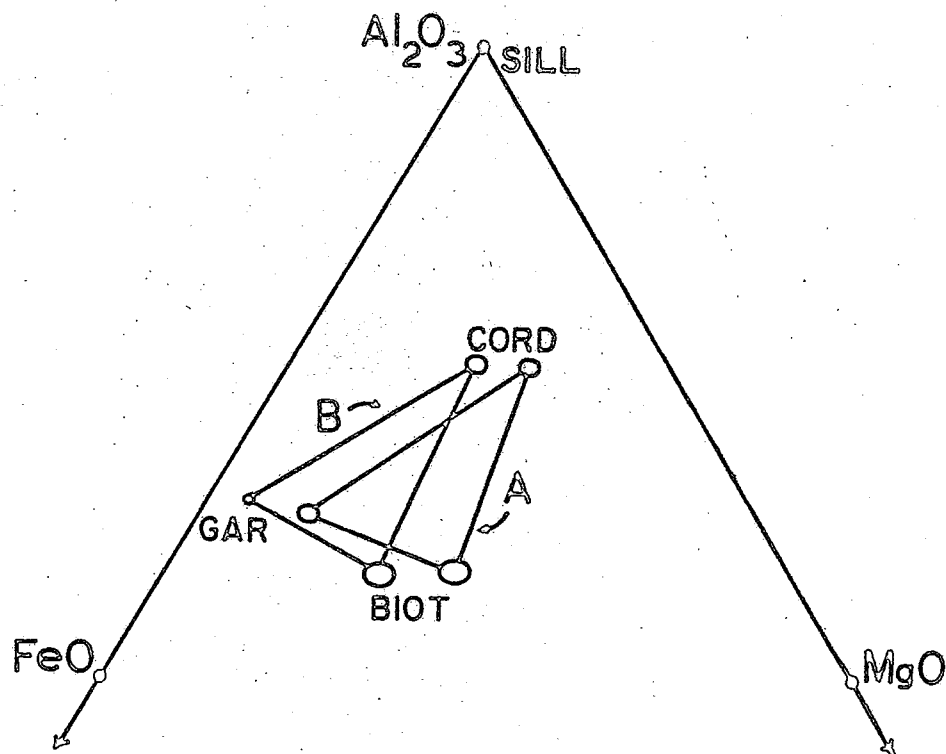
Figure 7. Diagrammatic comparison of limiting compositions in the regional (A) and outer aureole (B) assemblages. — Projected from K-feldspar and quartz (see text).

Choice of Assemblage for Comparison of Regional
and Outer Aureole Metamorphism

At least three phases of garnet, cordierite, biotite or

sillimanite can be assumed to have been compatible in the regional or

contact gneisses with K-feldspar, magnetite, quartz, and oligoclase.

If we arbitrarily choose an assemblage to be stable, e.g., garnet-

cordierite-biotite coexisting with the other phases excepting silli-

manite, we can show the effects of changes in T, P, and f_{O_2} upon it.

The compositional shifts of the phases can then be qualitatively pre-

dicted from experimental studies and studies of natural assemblages

without making any further assumptions as to their compatibility in

the Caribou aureole.

Theoretical Pressure Effect on Assemblage

Considering phase triangle A as our hypothetical assemblage,

decreasing pressure at constant temperature and f_{O_2} will shift the

phase compositions toward higher values of Fe/Mg (Currie 1971, fig. 2,

Ganguly 1972, fig. 5), while the change in Fe/Mg partitioning between

garnet-biotite and cordierite-biotite will be very small (Sen and

Chakraborty 1968, p. 39, Perchuk 1970, p. 160-161).

Theoretical Temperature Effect on Assemblage

An increase of temperature at constant pressure and f_{O_2} will

drive mineral compositions in the assemblage in the same direction as

decreasing pressure (Currie 1971), but partitioning between the three

phases will presumably approach unity. The net result is that the field

of garnet stability narrows (Chinner 1962, Perchuk 1970, Currie 1971).

Theoretical Effect of f_{O_2} on Assemblage

The effect of f_{O_2} on the assemblage can be demonstrated by balancing reaction 1. Ignoring anorthite, two Fe end-member reactions can be deduced:

Fe-Biotite + 1/2 O_2 = K-feldspar + Magnetite + Quartz + H_2O (3a)

and,

2 Almandine + 2/3 O_2 = Fe-Cordierite + 4/3 Magnetite + Quartz. (3b)
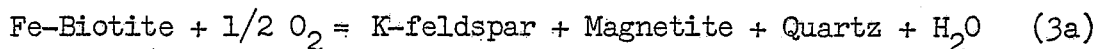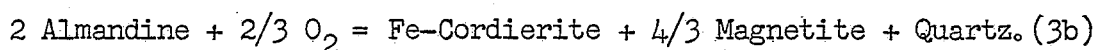
Equations 3a and 3b could be summed algebraically to a reaction similar to reaction 1 which would represent equilibration in the system containing only Fe^{2+}, and not Mg. Writing the reactions in this way it can be seen that a change in f_{O_2} could cause compositional changes: biotite and garnet will both change toward higher Mg/Mg + Fe with an increase in f_{O_2}. By writing the Mg-Fe exchange reaction between biotite and garnet it could be seen that Mg-Fe partitioning is only a function of P and T (and X).

Possible Causes of Assemblage Composition
and Partitioning Shifts

The foregoing analysis can now be compared with the data collected in this report and from previous workers. The compositional response (or appearance of a new mineral, e.g., cordierite) of the regional minerals, represented by A in figure 7, to the contact metamorphism which generated the compositions in triangle B could be due to changes in one or all of the intensive variables P, T, and f_{O_2}.

Temperature estimates made by Gable et al. (1970) for the
aureole from the heatflow models of Steiger and Hart (1967) fall in
the range between 400 to 600°C compared with Precambrian regional
temperatures of 630 to 710°C. The direction of change in Mg-Fe
partitioning as indicated in figure 7 is consistent with a lower
temperature in the contact event. A decrease in pressure from the
regional conditions is indicated by the observation that the Laramide
plutons were probably intruded as subvolcanic complexes at shallow
depth (Lovering and Goddard 1950, p. 40-42); an extensive throughgoing
hydrothermal system related to the intrusion at Caribou transects the
aureole. The compositional shift in the regional minerals apparently
reflects this drop in pressure. While there is no direct evidence to
indicate the values of f_{O_2} in the two environments, any rise in f_{O_2}
was masked by the effect of pressure on the garnet, biotite, and
cordierite compositions. Since magnetite is present in both assem-
blages, there is no need to assume that the contact environment in the
outer aureole was characterized by a much higher or lower f_{O_2} than
was the regional one.

The pressure effect on the regional minerals is probably simi-
lar to that described by Okrusch (1971) for the compositional shift
of the regional to the first contact assemblage in the outer Steinach
aureole. There, compositions of garnet and biotite are considerably
more Fe-rich in the contact assemblage than in the regional one, as
at Caribou. Cordierite appears as a new mineral in the contact

assemblage, whereas the regional assemblage is <u>quartz-sillimanite-biotite-garnet</u>. Gable et al. (1970) considered only the effects of temperature, f_{H_2O} and f_{O_2} in the Front Range aureoles.

Reaction Model

The low titania content of green biotite compared with initial matrix (brown) biotite, and its variable abundance within the pseudomorphs are evidence that it formed as an intermediate product during the breakdown of regional garnet. This, in turn, suggests that overall reaction 1 is not adequate to describe the reaction mechanism leading to formation of the cordierite pseudomorphs after garnet.

New mass balance expressions formulated to correspond to the kinetic steps might tell us more about the reacting system. Two component reactions in the system $SiO_2-Al_2O_3-TiO_2-FeO-MgO-CaO-K_2O-H_2O$ are written and discussed below using the compositional data such as are found in table II:

1.0 Garnet^{reg} + .47 K-feldspar + ν_{H_2O} H_2O → .51 Garnet^{eq} + .07 Cordierite + .57 Biotite (green) + .06 Anorthite (in plagioclase) + .93 Quartz   (4a)

and,

.51 Garnet^{eq} + .16 Biotite (green) + .20 O_2 → .27 Cordierite + .12 Quartz + .05 Anorthite + .14 K-feldspar + .40 Magnetite + ν_{H_2O} H_2O (4b)
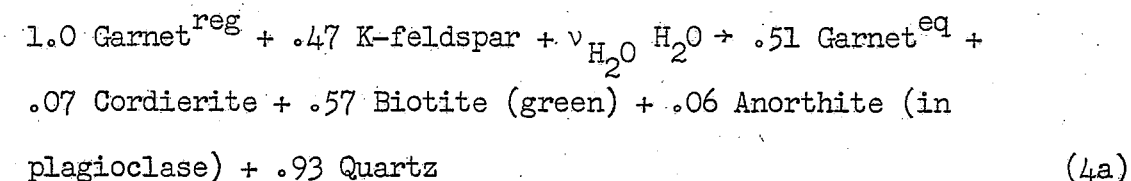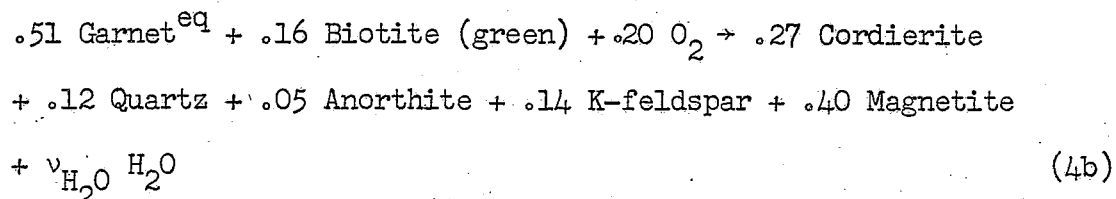
where "reg" = the garnet core composition, "eq" = apparently stable composition in system, and ν_{H_2O} is a reaction coefficient. The

reaction coefficients may only represent the process under one set of imposed conditions.

Reaction 4a is the irreversible reaction involving regional garnet out of equilibrium with the matrix. It is responsible for the production of green biotite and compositional shift of garnet, and results in garnets being zoned with respect to Mg, Fe, and Mn. In sample EC13 garnet is reacting to form green biotite, cordierite, and garnet rim. In this case, described by Loomis (1975), the flux of ions leaving the interface lies on the cordierite-biotite join, as implied by the compositional invariance of those minerals in contact with garnet core (cf. non-steady-state model, Loomis 1975). The reaction rate of garnet in reaction 4a is presumably limited by lattice diffusion in garnet because that mineral is internally zoned and the rim composition is invariant.

From reaction 4a we can deduce that K_2O (presumably actually from the breakdown of K-feldspar in the matrix to other products) and H_2O must diffuse into the pseudomorph while CaO and SiO_2 must leave, this assuming the Al_2O_3 is relatively immobile. The biotite formed reflects the limited interaction with the matrix in its having low Ti content.

Reaction 4b is based on the following criteria: 1) much, or all intermediate product (green) biotite disappears with greater reaction progress, and 2) garnet decreases in modal abundance below what is predicted in reaction 4a. Reaction 4b must be kinetically slower than reaction 4a. To react all of the garnet, a small amount

of brown matrix biotite must also be consumed. No other input from outside the pseudomorph, except perhaps of O_2, is necessary to write the reaction.

The balanced overall reaction is the algebraic sum of reaction 4a and reaction 4b:

$$1.0 \text{ Garnet}^{reg} + .33 \text{ K-feldspar} + \nu_{H_2O} \text{ H}_2\text{O} + .20 \text{ O}_2 \rightarrow$$
$$.34 \text{ Cordierite} + 1.05 \text{ Quartz} + .11 \text{ Anorthite} + .37 \text{ Biotite}$$
$$\text{(green)} + .40 \text{ Magnetite} \tag{5}$$
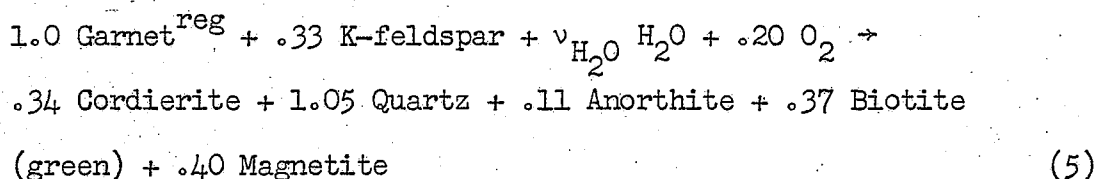
Ti shows some mobility. Analysis of greenish-brown biotite in a more completely reacted domain than is shown in figure 4a and figure 4b (fig. 4d) shows that Ti and Al approach matrix biotite values, suggesting that diffusion equalized μ_{Ti}^{Biot} and μ_{Al}^{Biot} between biotites with time. The stability of biotite was not apparently affected, though, by the rate of diffusion of these components.

The component reactions above do not demonstrate that diffusion of chemical components was restricted to the pseudomorph and immediate surroundings. Plagioclase (a product), e.g., is not immediately available in a few of the pseudomorph areas or as inclusions in regional garnet. However, variation in product phase abundance not correlated with extent of reaction is as easily explained as being due to kinetic factors (such as different reaction rates for reactions 4a and 4b) as it is by postulating a more completely open system. The proposed reactions, as written, also do not allow quantitative comparison with the actual modal percentages of product minerals in the

pseudomorphs because such calculations are subject to large errors
in 1) modal analysis, and 2) assumptions about the size of the original
garnet.

Problem of Determining Mechanism in Disappearance
of Green Biotite

Zoning and compositional invariance of garnet rims implies
that lattice diffusion in garnet controlled the rate of reaction 4a.
In a complete model for the overall reaction, however, we would like
to know what factor or process controlled reaction 4b, the reaction of
garnet rims with green biotite. The importance of diffusion and
diffusion rates is proven by the nature of the products and their
compositions formed by reaction 4a above. Intergranular diffusion
may also have been important in localizing the products to the
vicinity of garnet to form pseudomorphs and in forming the textures
resembling systematic zoning within the pseudomorphs, such as the
regular occurrence of magnetite along cracks flanked by biotite and
cordierite separating it from garnet.

The reaction of garnet rim with biotite (green or brown) in
equation 4b is dependent on f_{O_2} and f_{H_2O}, which presumably could con-
trol reaction rate and mineral compositions. An attempt was made to
relate biotite and cordierite compositions measured to their locations
in the pseudomorphs, particularly as to their proximity to garnet.
Consideration of all the data from two domains and of data collected
in separate probe runs shows that: 1) the Mg/Mg + Fe ratio in

biotite and cordierite are higher away from garnet, and 2) that the highest ratios are for pairs measured next to magnetite, even where close to garnet.

The variation in $Mg/Mg + Fe$ ratio can be either a function of 1) the flux supplied by garnet by reaction 4a, 2) of higher f_{O_2} away from garnet, or 3) of incomplete equilibration in the pseudomorph. The first possibility should not be important assuming diffusion in garnet of the type described above, unless the intensive variables were not constant during the reaction time. In the second case, the mobility of O_2 in metamorphic rocks is known to be low. If enough O_2 was consumed at the garnet interface, f_{O_2} might have decreased and the reaction stopped. Thus, while control of f_{O_2} external to the pseudomorph seems unlikely, variation of f_{O_2} away from garnet remnants seems certainly possible. The f_{H_2O} could have varied also as a function of changing conditions in the aureole, and conceivably changing f_{H_2O} in the pseudomorph could explain the compositional differences.

The discussion above can be advanced no further in any case, and unfortunately the data lack desirable precision because of the limited number of analyses collected. If the compositional variations are real, the data do not rule out the possibility that the diffusion rate of O_2 or changing f_{H_2O} could have controlled the rate of reaction 4b. Alternatively, however, nucleation and interface-controlled growth of euhedral magnetite could have controlled the rate of the reaction (cf. McLean 1965). The data, unfortunately, give no proof as to whether diffusion of oxygen or surface effects controlled the reaction rate.

ANALYSIS AND INTERPRETATION OF REACTIONS INVOLVING BIOTITE AND SILLIMANITE TO PRODUCE CORDIERITE IN THE INNER AUREOLE

Disappearance of Garnet in Inner Aureole

In the inner aureole, garnet is no longer present. In one thin section (CB8) from the inner aureole, pseudomorphs after garnet consist of cordierite, magnetite, quartz and fine-grained K-feldspar(?). While garnet is stable relative to cordierite with increasing temperature, with increasing f_{O_2} such products as described above from the breakdown of garnet are expected (Ganguly 1972). Evidence from other contact aureoles (Chinner 1960, 1962; Okrusch 1971) and experimental data (e.g., Hsu 1968) indicate that spessartite-rich garnet could be stable in the similar P, T, f_{O_2} environment of the inner aureole. Perhaps not enough Mn was available to stabilize that phase.

Description of Sample

While oxidation of garnet to produce cordierite characterizes the outer aureole, continuous reaction of biotite and sillimanite to form cordierite in increasing abundance characterizes the inner aureole. The reaction was only observed in thin sections where garnet is absent, and its initiation is apparently abrupt in the Caribou aureole. Figure 8 is a photomicrograph of a domain of reaction in sample CB7 from the inner aureole. Euhedral magnetite, ragged prisms of sillimanite, and rounded biotite grains are included in large crystals of cordierite. K-feldspar (orthoclase) in large,

39
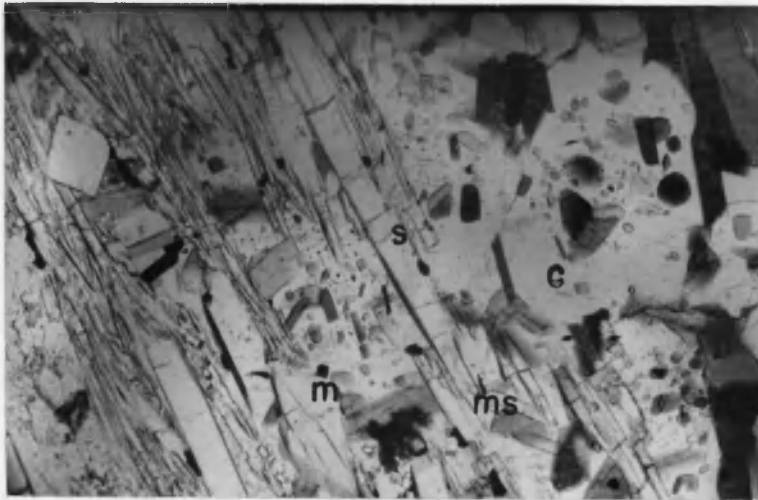
Figure 8. Photomicrograph of a reaction domain in sample CB7. —
Plane-polarized light. 65X. Shows breakdown of biotite
and sillimanite to form cordierite, magnetite, ilmenite
(not shown) and muscovite. Note rounded biotite remnants
and sillimanite in cordierite.

anhedral grains, and/or muscovite altering biotite crystals outside

the cordierite, and a small amount of ilmenite ($Ilm_{90}Hem_{10}$) in

anhedral grains are also present in the domain. From consideration

of the textures, cordierite appears to have been produced by the

general (unbalanced) reaction:

$$\text{Biotite + Sillimanite + Quartz} + O_2 \rightarrow \text{Cordierite + Ilmenite}$$
$$+ \text{Magnetite}_{SS} + \text{K-feldspar} + H_2O \tag{6}$$
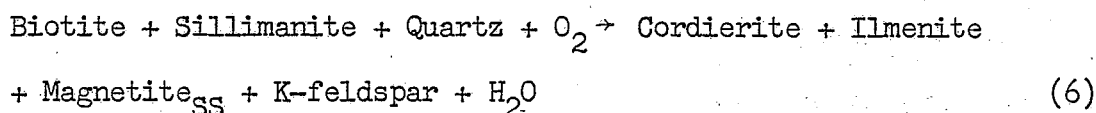
(cf. Gable et al. 1970).

Analytical Results

Analytical Data

     Analysis of the reacting system involving sillimanite, biotite,

and cordierite can be performed in the same manner as for the garnet

pseudomorphs. Two partial analyses of cordierite and biotite are

listed in table II, and all of the data collected in a single domain

of reaction are projected from K-feldspar and quartz in figure 9 with

tie lines between analyzed mineral pairs. Biotites show small, but

significant, compositional variation. Those biotites with low Fe/Fe

+ Mg ratios are large crystals corroded by cordierite; and, conversely,

the small, rounded inclusions in cordierite are Fe-rich. This trend

was confirmed by analyzing cordierites and biotites from three other

reaction areas in CB7, including one where reaction was incipient.

The symbol, $\mathcal{C}$, in figure 9 illustrates the findings from the texture

and composition data that progressive reaction results in more
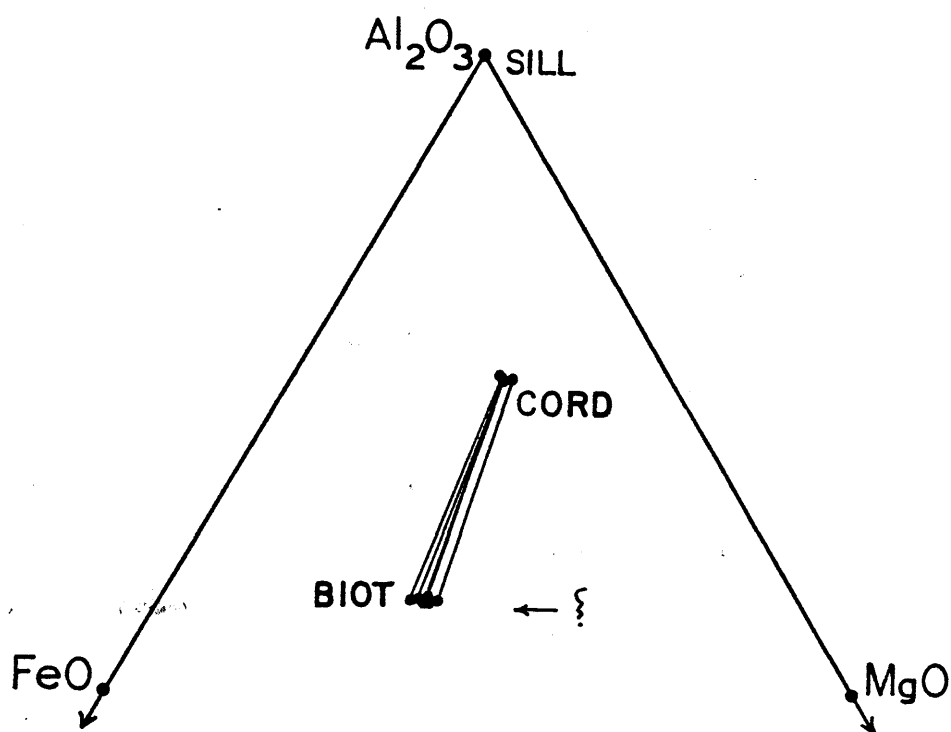
Figure 9. AFM projection from K-feldspar of probe analyses of biotite and cordierite in CB7. — Analyses are from a single reaction domain and tie lines connect rim compositions of minerals in direct contact. The symbol denotes increasing extent of reaction as determined texturally.

Fe-rich biotites, and perhaps more Fe-rich cordierite. One biotite "armored" by quartz and embayed by plagioclase was analyzed for purposes of comparison with the finding that Fe/Fe + Mg is the same as for the small biotite remnants in cordierite.

Projection of the Final Assemblage

The stable equilibrium assemblage would appear to be quartz-(Fe-rich) biotite-sillimanite-(Fe-rich) cordierite-K-feldspar-magnetite-ilmenite. The data do not indicate whether or not the assemblage mineral compositions represent equilibrium values. It is possible that the changes in composition merely reflect changes in bulk composition within a domain. Figure 10 is a graphical comparison of biotite and cordierite analyses from the outer and inner aureoles (samples EC13 and CB7, respectively). The filled circles represent the final inner aureole compositions and show a trend toward higher Mg/Mg + Fe approaching the igneous contact. The two sets of data can be compared if it is assumed that pseudomorph biotite-cordierite pairs away from garnet (in the outer aureole) are a separate sub-system not including that mineral, but including sillimanite.

Causes of Compositional Shifts

One variable likely to have differed in the inner compared to the outer aureole is temperature. However, the opposite compositional shift was noted by Okrusch (1971) for biotite and cordierite in the Steinach aureole, where simply temperature, and not increasing oxidation, was involved. f_{O_2} seems to have increased toward the
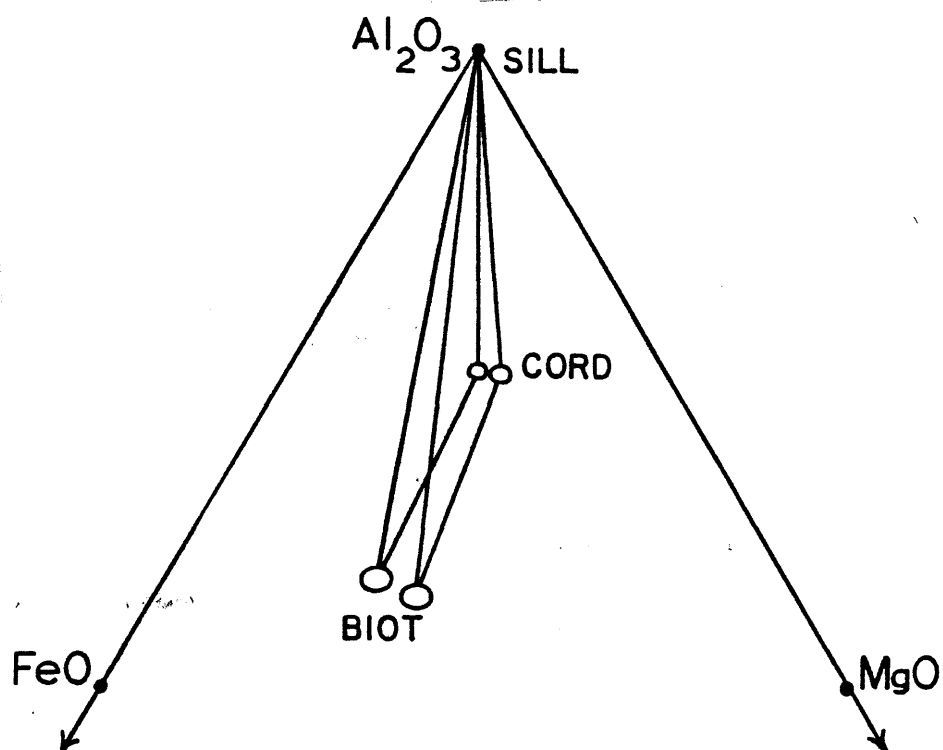
Figure 10. Diagrammatic comparison of limiting "equilibrium"
compositions of biotite and cordierite in outer aureole
(EC13, left) and inner aureole (CB7, right).

contact. This follows from the fact (Ganguly 1972) that the coexistence of cordierite, sillimanite, magnetite, and quartz (3 Cord + O_2 = 6 Sill + 2 Mag + 9 Qtz) as was observed in the inner aureole defines a higher f_{O_2} than that in equilibrium with cordierite, almandine, magnetite and quartz (54 Alm + 18 O_2 = 27 Cord + 36 Mag + 27 Qtz), observed in the outer aureole. Implicit in this reasoning is the assumption that cordierite and sillimanite are in equilibrium in the inner aureole; this cannot be confirmed by the data. However, the fact that Mg/Fe ratios in biotite and cordierite are higher in the inner aureole is also evidence of higher f_{O_2} there.

Discussion

Variation or gradients in intensive variables over the thin section can explain different extents of reactions between separate domains but may not explain compositional variation of biotite and cordierite <u>within</u> a single domain. The data show that cordierite and biotite could not have simply reacted by Mg-Fe exchange, although K_D (related to slopes of the tie lines) does reflect the nature of the assemblage disequilibrium.

Control of the Reaction

Diffusion in biotite did not evidently control the reaction rate. Biotite grains are either homogeneous or slightly zoned, but only the small grains have the assumed equilibrium rim composition. The dissolution rate of biotite or sillimanite could have been the rate-controlling factor, however. If dissolution at the interface of

a reacting grain is slow compared to diffusion of ions in the grain itself, a zoning profile will not develop. Alternatively, consumption of internally controlled O_2 in the reacting system could also have limited reaction rate and have been responsible for increasing Fe/Fe + Mg in biotite with greater extent of reaction. The compositional data are insufficient to distinguish which process controlled the reaction rate; the intergranular diffusion model does not explain, however, the random distribution of product phases observed in thin section and the fact that compositions of cordierite and biotite bear no relation to distance from sillimanite.

APPLICATION OF RESULTS

The oxidation reactions described here have immediate significance to stable isotope geology. Shieh and Taylor (1969, p. 333) measured mineral isotopic (O^{18}/O^{16}) temperatures in pelites from the Caribou and Bryan Mountain (Eldora) stocks. These authors state: "The schists and gneisses in the Caribou and Eldora traverses give rather high quartz-biotite temperatures (630 to 710°C) for samples 1000 feet away from the contact, but the quartz-magnetite temperatures (595 to 615°C) seem more reasonable, and these conceivably could represent the original metamorphic temperatures." For the samples in question (which had not undergone oxygen isotopic exchange with the intrusion), an explanation for the discordant temperatures should be obvious from consideration of the data presented here. While much, or most of the magnetite in the pelites formed (or equilibrated) during contact metamorphism from the breakdown of biotite and/or garnet, abundant unreacted biotite is preserved in many rocks which may reflect the regional temperatures. Because H_2 was released or consumed by the reactions taking place in the aureole, D/H isotopic ratios should also be interpreted with considerable caution (Gable et al. 1970, p. 685).

CONCLUSIONS

The author has shown in the foregoing analysis that the
nature of the contact metamorphism can be understood despite complex
changes in the intensive variables. Previous work centered on the
Front Range aureoles (Gable et al. 1970) demonstrated that T, f_{O_2},
and f_{H_2O} were controlling variables of metamorphism. Detailed
analysis of the mineral phases in the pseudomorphs and construction of
an equilibrium topology forces recognition of pressure as an impor-
tant variable. The inner aureole also was more oxidizing than the
outer aureole.

Other results were obtained which hinge less on the assump-
tion of complete or partial equilibrium and more on the textural
interpretations and microprobe analyses of minerals involved in the
reactions studied. The data permit deduction of the reaction
kinetic path because intermediate products are formed (component
reactions 4a and 4b). This yields more information than can be
obtained by writing reactions based on textural abundances or associa-
tions alone, or by merely writing the overall reaction for the
breakdown of garnet (reaction 5). The component reactions are useful
in comparing ion mobilities during intergranular diffusion: e.g.,
Ti diffuses more slowly than does K_2O and H_2O, otherwise we wouldn't
have green biotite. Immediately obvious net gains and losses in the
pseudomorph include that of K_2O, H_2O, TiO_2, and of SiO_2 and CaO,
respectively.

Reaction 4b, for some reason, is slower than reaction 4a. The limiting factor in reaction 4a is probably lattice diffusion within garnet; and, if the diffusion constants for this process were known, the rate of reaction 4b would also be known, and thus also the maximum rate at which the breakdown of garnet takes place. The rates of intergranular transport of components, as exemplified by reaction 4b, are parameters necessary to the interpretation of equilibrium volumes in metamorphic rocks and moss transfer. The data do not indicate the reaction mechanism of reaction 4b nor of the breakdown of sillimanite in the inner aureole to cordierite and other products. Whether intergranular or lattice diffusion, or interface-controlled mechanisms limit reaction rate must be determined for any metamorphic reaction at the conditions under which they take place. With this information, the time of metamorphism of a sample and the rock units in which they are contained could be calculated.

APPENDIX I

SAMPLE COLLECTION

Previous workers provided a geologic map base upon which
sampling was carried out. The units present around the Caribou stock
include microcline gneiss, hornblende gneiss, pelitic gneiss, and
Precambrian intrusive plutonic and dike rocks (Gable 1969 and fig. I.1).
Pelitic gneisses on the western and eastern contacts of the stock
correspond to the northwest and northeast limb, respectively, of a
northeast–plunging Precambrian anticlinal structure.

Several faults of unknown magnitude of displacement are shown
on the published map (Gable 1969) in the vicinity of the sampling
area, but only one of these, a northwest–trending break which follows
the creek (fig. I.2) draining Caribou transects the sample grid. A
thorough search failed to confirm the presence of the northwestern–
most extension of this fault as drawn by Gable. No breccia, staining,
or change in lithology or structural trends was noted in outcrop or
near–outcrop along the inferred trace of the fault in the sampling area.

Cross–sections were constructed for two of the sampling lines
from structural data collected along the traverses. Figure I.3 (B–B'
in fig. I.1) depicts the structure on the west end of the stock from the
south side of Klondike Mountain. The gneisses in the aureole from
sample locations marked 1 to 8 (fig. I.2) are well–foliated pelitic and
semi–pelitic gneisses with a granitic component as thin veins parallel
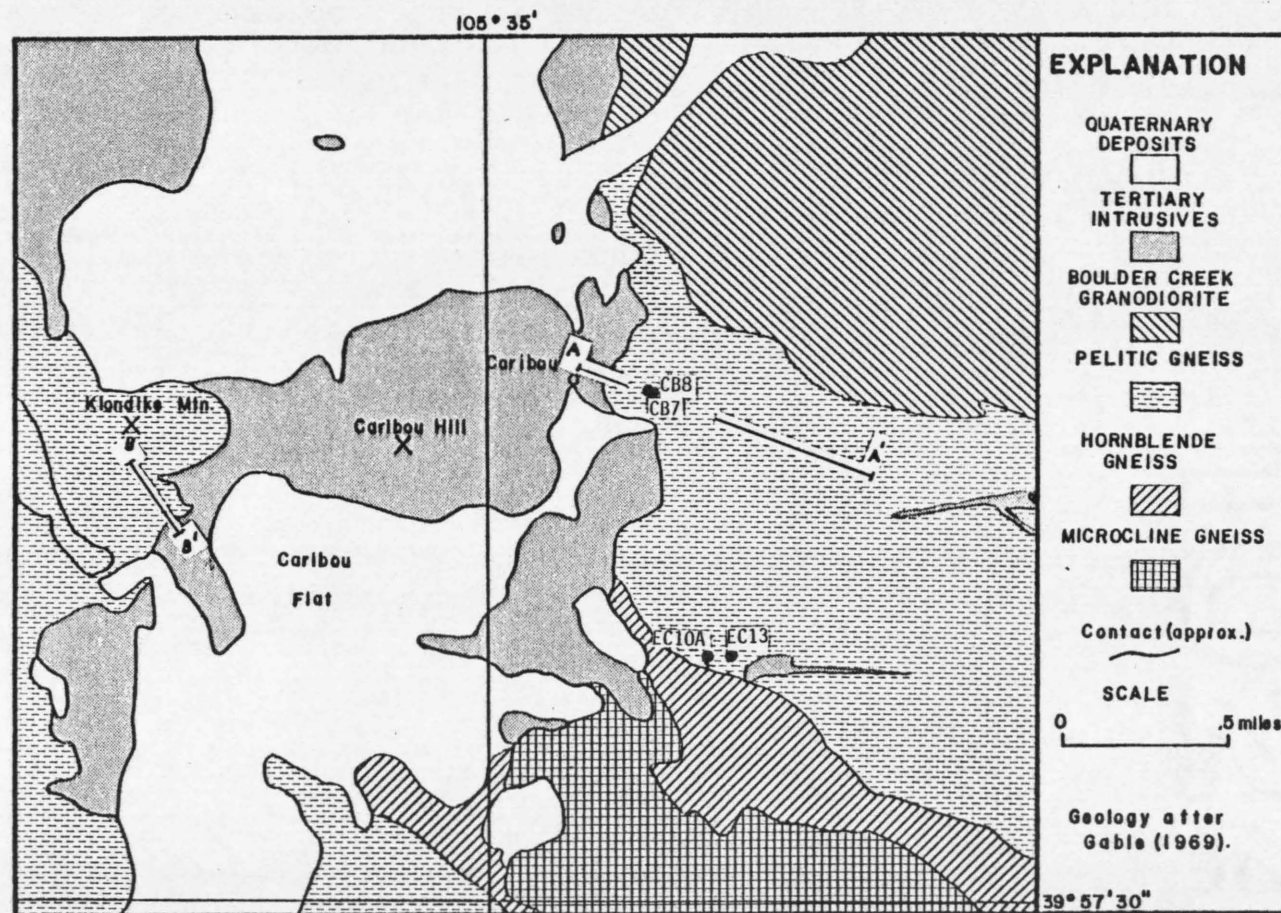
Figure I.1. Map of geologic units and structure section locations.
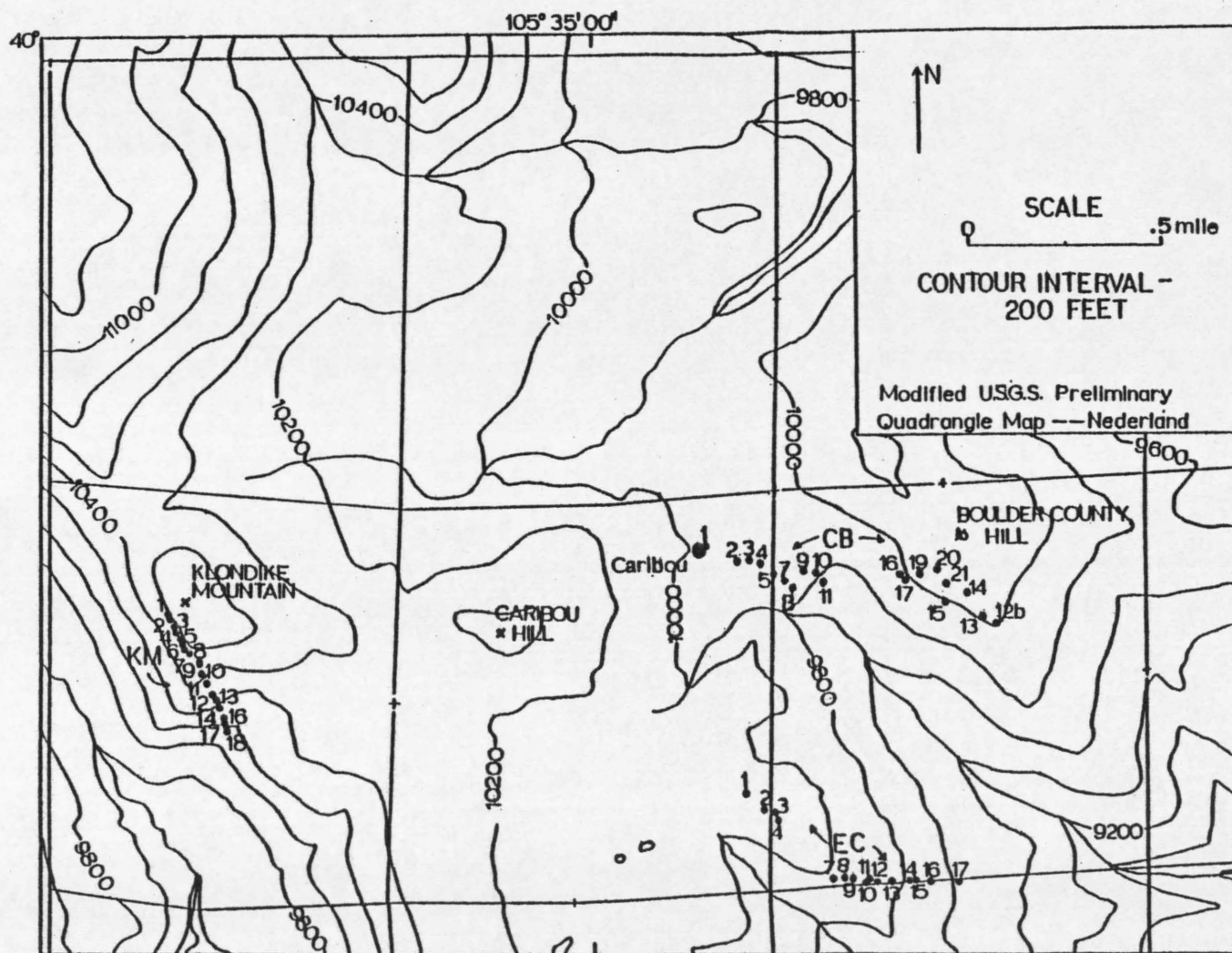
Figure I.2. Sample location map. — Only selected samples are shown.
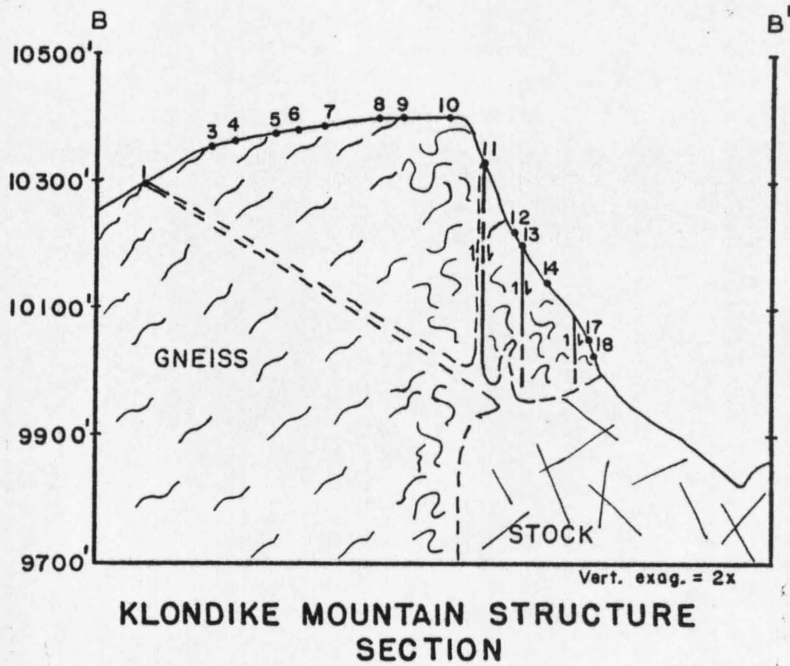
Figure I.3. Schematic structure section of geology south of Klondike Mountain. — Sample locations are projected onto the plane of section.

to foliation, and occasional folded pegmatite lenses. At sample location 9, the regional foliation becomes swirled and offset slightly by steep-dipping fractures. Platy parting found in the less disturbed rocks (e.g., locations 1 to 8) is healed; foliation is less pronounced, and the rock matrix is more homogeneous in appearance.

Several near-vertical dikes are drawn in schematically or where they were noted at a sample location. These occupy a well-developed fracture system seen on the scale of the hand specimen (above) and in outcrop, along which slippage east-side down has taken place. Some of the dikes pinch out upwards and the foliation in the gneiss is kinked above the dike apices. Toward the contact near the base of the cliff face large blocks of gneiss are surrounded by coarser, dark grey monzonite.

The western contact of the Caribou stock thus appears to have intruded passively and to have involved downward stoping of the roof and walls into the magma. The amount of disturbance in aureole rocks increases toward the contact gradationally and involves no major internal displacements. Because exposure is nearly complete, and because the topography affords a natural cross-section through the roof, a more detailed study of the intrusion emplacement could be undertaken.

Unfortunately, the surface expression of the contact relations on the east side of the stock near Caribou is not as good. The slopes and ridgetops are partially forested and are covered with a thin veneer of colluvium, and stream deposits blanket the valley below

Caribou townsite. A rough cross-section (A-A') is shown in figure I.4.
The gneisses are lithologically similar to those in the western
aureole but contain more abundant folded pegmatite, assumed to be
Precambrian. Two varieties were noted: 1) those predominantly micro-
cline and quartz, and 2) those containing quartz, K-feldspar, plagio-
clase, and biotite. Foliation conforms generally to the same
northwest strike and northeast dip except near the intrusive contact.

The exposures of the contacts are only fair. Dikes and
fractures along which slippage took place are not characteristic of
the gneisses near Caribou townsite. The wall-rock in the Idaho
tunnel and in the Caribou Mining Company mine operated by Mr. T.
Hendricks 150 yards to the south (shown on map by Gable 1969) is
apparently gneiss for a considerable distance (T. Hendricks, oral
communication, 1975) inward. The data indicate that the section
represents a portion of the aureole below the roof, and that the stock
is steep-sided.

A throughgoing vein system traverses the Caribou stock and
portions of the pelitic rocks, and was mapped and discussed by
Lovering and Goddard (1950). Those authors assumed that its orienta-
tion was controlled by Laramide tectonic forces, but Tweto and Sims
(1963) contend that Precambrian fractures already present in the rocks
may simply have been reactivated during the later events. Sulfide
mineralization of the veins produced workable amounts of silver and
base metals (in the 19th century) mostly within the zone of supergene
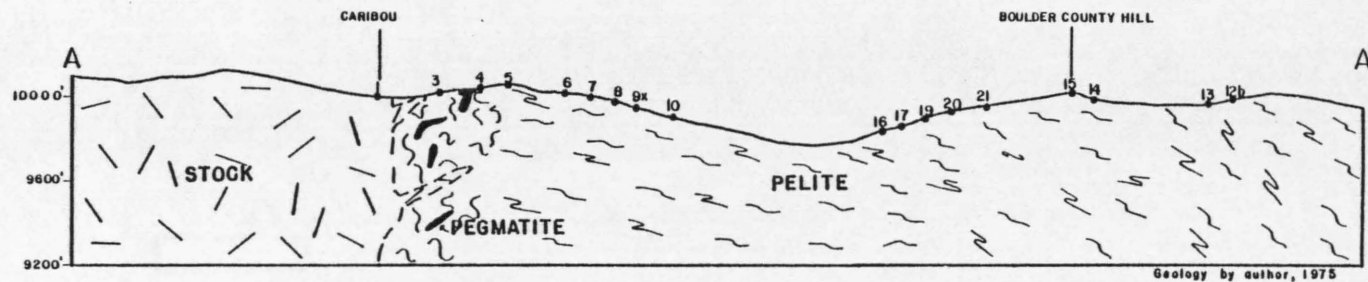
EAST CARIBOU TRAVERSE AND STRUCTURE SECTION

SCALE

Figure I.4. Schematic structure section of geology east of Caribou along sampling line. — Sample locations are projected onto the plane of section.

enrichment. Mineable ore gave out at moderate depth, but there has been intermittent interest in the larger east-west trending veins up to the present day.

The relations between the veins and wallrock alteration were investigated briefly from outcrops and prospect pits in the field. The veins have sharp planar contacts with the pelitic host gneisses where they are relatively unfractured and are filled with brown, gouge-like, soft material and stringers of quartz. Near mine shafts and clusters of pits, the gneisses themselves are broken, and abundant white quartz forms part of the surface veneer. Where outcrops are present, alteration of gneiss can impart a crumbly fracture when struck with a hammer. Micaceous layers are rusty-colored and the feldspars appear clouded. Distinct veinlets are largely lacking in these outcrops except in the unexposed broken areas near veins; rather a system of fractures sometimes coated with epidote, muscovite, and oxide minerals appears to be responsible for the incomplete, but pervasive alteration. In a sense, then, a "halo" of alteration which is grossly discernible characterizes intersections and concentrations of veins. The area east of sample no. 10 in figure I.3 (the small basin and Boulder County Hill) is greatly affected by vein-related alteration.

Sampling Technique

Samples were collected from outcrops only and their locations were plotted on the U.S.G.S. 7.5 minute preliminary topographic map of the Nederland Quadrangle or on the geologic map of Gable (1969).

Absolute distances between samples were determined both by pace and compass from landmarks or triangulated points. Attempts were made to sample different bulk compositions in a given outcrop where possible, and also to avoid any obvious proximity to dikes and veins. Portions of several days were spent in investigating the structural character-istics of the aureole and the Caribou stock. The time spent sampling was in two periods separated by an interval of thin section examina-tion at the University of Arizona.

Sample locations are shown in figure I.2, an overlay of the topographic map. Two of the traverses (KM and CB series) are projected onto the cross-sections (figs. I.2 and I.3). Several scattered samples from the aureole and from a traverse across the stock are not shown because they were not studied in detail.

Sample Paragenesis

The sampling experience of the author may aid further investigations. Bulk compositions are limited in range in the vicinity of Klondike Mountain. Garnet was found in only one badly altered sample, although most of the samples collected were very fresh. Cordierite appears in most of the rocks at about the point where foliation becomes swirled (sample KM9, above), and along with K-feldspar becomes an abundant constituent at the expense of biotite. Andalusite is present in thin sections cut from samples located between 500 and 1000 feet from the contact (Gable et al. 1970). Muscovite is present in large crystals in all of the samples

containing cordierite. The alteration mineral assemblage appears to comprise sericite, quartz, chlorite (var. penninite), calcite, and hematite.

Samples from two traverses on the east side of the stock, CB and EC, are more diverse mineralogically in that some contain garnet. Usually red or dark-colored in hand specimen, garnet generally shows up as knots in the foliation planes of the gneisses. Not a single garnet-bearing sample from the CB traverse was deemed suitable for study because of the pervasive quartz-sericite-chlorite-opaque oxide alteration in most of the samples which obliterated original textures. An area of no outcrop separates the outer from the inner aureole where no fresh samples were found. Pseudomorphs after garnet in samples CB7 and CB8 discussed in the text were identified as garnet in outcrop. Andalusite was found in two thin-sectioned samples at greater than 1000 feet from the igneous contact. The mineral appears to be growing poikilitically with, or on, quartz, and is associated with a new generation of biotite.

Samples from the EC traverse afford the only known exposures of fresh garnet-bearing rocks around Caribou. Even here, few outcrops contain many layers with garnet, and some are deeply surface-weathered. Unfortunately, topography dictated the traverse direction such that the significance of relative distances between samples must be deduced from the CB traverse.

APPENDIX II

TABLES OF CHEMICAL ANALYSES

Table II.1. Sample EC13 — biotites.

Sample* and Lab #**	1 UWG11	2 UWG12	3 UWG13	4 UWG14	5 UCG1A	6 UCG1A2	7 UCG1K	8 UCG1N	9 UCG1P	10 UCG2M	11 UCG2N	12 UCG2O	13 UCG3R	14 UCG3S	15 UCG4A	16 UCG4C	17 UCG4E	18 UCG4G	19 UCG5
SiO_2	37.39	36.63	36.24	35.80	34.49	34.74	34.39	34.59	34.58	35.17	34.99	34.52	35.02	33.95	34.64	34.46	35.09	34.40	34.44
Al_2O_3	18.81	20.94	18.82	20.38	21.06	20.56	20.73	20.32	20.89	18.73	18.62	18.68	20.88	20.51	19.80	19.82	20.12	19.73	20.51
TiO_2	3.31	.14	4.14	1.81	.09	.08	.21	.10	.12	2.84	2.82	2.32	.63	.81	2.42	1.42	.10	2.56	.76
FeO_t	22.74	23.37	23.95	22.34	25.40	23.53	23.55	23.21	23.61	23.46	22.95	23.72	23.29	23.30	22.99	23.18	23.53	22.79	22.82
MnO	.21	.15	.23	.26	.16	.15	.15	.13	.12	.22	.20	.26	.13	.14	.20	.21	.11	.17	.16
MgO	6.70	7.13	6.13	5.93	7.76	6.94	6.73	7.40	7.08	6.78	6.57	7.06	6.82	6.62	6.55	7.00	7.41	6.54	6.61
CaO	.01	.05	0.0	.01	.18	.12	.09	.12	.12	.13	.19	.14	.08	.08	.08	.08	.05	.08	.09
Na_2O	.26	.36	.22	.24	.29	.29	.34	.33	.35	.24	.23	.21	.31	.26	.26	.31	.29	.27	.35
K_2O	9.12	8.64	9.30	8.98	8.48	9.29	8.88	8.92	8.75	9.02	8.97	8.76	9.02	8.94	9.15	8.92	9.18	9.05	8.79
H_2O	1.41	2.54	.76	4.15	2.06	4.24	4.88	4.79	4.32	3.36	4.40	4.28	3.77	5.32	3.87	4.52	4.06	4.37	5.40
Total	99.96	99.95	99.79	99.90	99.97	99.94	99.95	99.91	99.94	99.95	99.94	99.69	99.82	99.79	99.76	99.71	99.83	99.79	99.77
Color	Brown	Green	Brown	Inter.	Green	Green	Green	Green	Green	Brown	Brown	Brown	Green	Green	Brown	Brown	Green	Brown	Inter.

*1 — Brown biotite on edge of pseudomorph away from cordierite.
2 — Green biotite touching garnet rim and cordierite (UWG11) inside pseudomorph.
3 — Brown biotite appearing encased in sillimanite in matrix.
4 — Brownish-green biotite on edge of pseudomorph touching cordierite.
5 — Green biotite touching garnet rim inside pseudomorph.
6 — Green biotite touching garnet rim inside pseudomorph.
7 — Green biotite touching cordierite (UWG13) inside pseudomorph, halfway to edge.
8 — Green biotite touching cordierite inside pseudomorph.
9 — Green biotite touching cordierite inside pseudomorph.
10 — Brown biotite in matrix, center of grain next to quartz.
11 — Brown biotite in matrix, closer to edge of same grain.
12 — Brown biotite in matrix, edge of same grain.
13 — Green biotite touching garnet rim, center of pseudomorph.
14 — Green biotite away from garnet; large grain in center of pseudomorph.
15 — Brown biotite touching cordierite near edge of pseudomorph.
16 — Small brown biotite in cordierite at edge of pseudomorph.
17 — Biotite next to cordierite and magnetite in crack in garnet remnant inside pseudomorph.
18 — Brown biotite at edge of pseudomorph touching cordierite.
19 — Brownish-green biotite next to cordierite in center of small pseudomorph.
**First two letters of title identifies laboratory (UW = University of Wisconsin, Madison, UC = University of California, Los Angeles, UA = The University of Arizona).

Table II.2. Sample EC13 — cordierites.

Sample* and Lab #**	1 UWG11	2 UWG12	3 UWG13	4 UWG14	5 UCG1A	6 UCG1J	7 UCG1D	8 UCG4B	9 UCG4D	10 UCG4F	11 UCG4H	12 UCG5	13 UCG1M	14 UCG1O	15 UCG1Q	16 UCG1R
SiO_2	50.40	50.61	50.19	50.37	47.83	47.80	47.42	47.87	48.55	48.70	48.25	48.26	48.43	48.45	48.25	48.12
Al_2O_3	32.46	32.65	32.72	32.64	32.73	32.05	32.80	30.78	31.93	31.85	31.04	30.53	32.40	31.20	31.56	31.94
TiO_2	.02	.02	.03	.03	.01	0.0										
FeO_t	11.06	10.69	10.90	11.25	11.63	11.45	11.83	11.23	11.11	11.78	11.12	11.15	11.68	11.32	11.56	10.59
MnO	.44	.56	.54	.52	.50	.48	.46	.51	.62	.46	.52	.50	.51	.42	.46	.63
MgO	5.44	5.72	5.47	5.47	6.30	6.14	5.86	6.53	6.52	6.46	6.56	6.48	6.43	6.50	6.36	6.70
CaO	.01	.01	.02	.02	.16	.12	.19	.09	.10	.10	.12	.11	.13	.13	.13	.11
Na_2O	.24	.20	.18	.18	.16	.09										
K_2O	.07	.08	.06	.07	.06	.06										
H_2O																
Total	100.14	100.54	100.11	100.55	99.38	98.19	98.56	97.01	98.83	99.35	97.61	97.03	99.58	98.02	98.32	98.09

*1 — Cordierite touching biotite (UWG12) and garnet in pseudomorph center.
2 — Cordierite touching biotite (UWG14), pseudomorph edge.
3 — Cordierite touching biotite (UCG1K), halfway to pseudomorph edge.
4 — Cordierite touching garnet (UWG14) inside pseudomorph.
5 — Cordierite touching garnet inside pseudomorph next to garnet.
6 — Cordierite in center of pseudomorph.
7 — Cordierite inside pseudomorph next to garnet.
8 — Cordierite touching biotite (UCG4A).
9 — Cordierite touching biotite (UCG4C).
10 — Cordierite touching biotite (UCG4E).
11 — Cordierite touching biotite (UCG4G).
12 — Cordierite touching biotite (UCG5).
13 — Cordieriet touching garnet (UWG15).
14 — Cordierite touching biotite (UCG1N).
15 — Cordierite touching biotite (UCG1P).
16 — Cordierite at edge of pseudomorph.
**First two letters of title identifies laboratory (UW = University of Wisconsin, Madison, UC = University of California, Los Angeles, UA = The University of Arizona).

Table II.3. Sample EC13 — garnets.

Sample* and Lab #**	1 UWG11	2 UWG12	3 UWG13	4 UWG14	5 UWG15	6 UCG1G	7 UCG1C	8 UCG1E	9 UCG1K	10 UCG3P	11 UCG3Q
SiO_2	36.60	35.98	36.67	36.57	36.48	38.49	38.58	37.06	38.54	38.73	37.65
Al_2O_3	21.66	21.08	20.71	20.44	20.40	21.44	21.38	21.93	21.14	21.97	21.06
TiO_2											
FeO_t	32.00	33.89	35.10	34.03	34.40	32.64	34.00	34.72	32.97	33.31	34.13
MnO	.93	4.91	1.70	4.92	5.55	.97	1.14	1.17	.97	1.04	6.36
MgO	5.85	1.48	3.50	1.50	1.55	5.86	5.56	1.65	5.72	5.65	1.42
CaO	1.60	1.28	1.40	1.26	1.38	1.72	1.73	1.80	1.42	1.48	1.31
Na_2O											
K_2O											
H_2O											
Total	98.64	98.62	99.08	98.72	99.76	101.12	102.39	98.33	100.76	102.18	101.93

*1 — Large garnet, core.
 2 — Same garnet, rim, touching biotite (UWG12).
 3 — Small garnet, core.
 4 — Rim of (3), touching cordierite (UWG14).
 5 — Small garnet core, next to cordierite (UWG1M).
 6 — Same as (1), above.
 7 — Narrow garnet, core.
 8 — Garnet core.
 9 — Large garnet, core.
10 — Large garnet, core.
11 — Large garnet, rim of (10).
**First two letters of title identifies laboratory (UW = University of Wisconsin, Madison, UC = University of California, Los Angeles, UA = The University of Arizona).

Table II.4. Sample CB7 — biotites.

Sample* and Lab #**	1 UWG25	2 UWG1C	3 UWG1D	4 UWG1G	5 UCG1X	6 UCG1W	7 UCG1L	8 UCG3A	9 UCG3D	10 UCG3E	11 UCG5	12 UCG6
SiO_2	37.50	36.61	37.57	37.87	35.87	35.84	35.03	35.09	35.24	35.05	35.28	34.91
Al_2O_3	19.41	19.14	18.69	18.63	19.24	18.43	18.52	18.77	18.80	18.17	18.46	18.40
TiO_2	2.72	2.86	3.06	2.66	2.67	3.48	1.19	1.20	1.38	1.00	1.08	1.09
FeO_t	19.55	21.17	21.13	20.58	20.44	21.39	20.81	20.22	20.20	21.39	20.46	21.12
MnO	.10	.08	.09	.08			.11	.12	.11	.10	.09	.11
MgO	7.64	8.38	8.30	9.03	8.31	7.87	8.41	8.45	8.53	7.79	8.85	7.93
CaO	0.0	0.0	0.0	0.0	0.0	0.0	.16	.13	.13	.13	.08	.16
Na_2O	.18	.21	.20	.22	.24	.19	.57	.54	.51	.61	.44	.60
K_2O	9.47	9.16	9.13	8.94	9.44	9.31	9.32	9.23	9.15	9.22	9.48	9.47
H_2O	3.37	2.37	1.81	1.97	3.76	3.45	5.81	6.18	5.87	6.46	5.70	6.13
Total	99.94	99.98	99.98	99.98	99.97	99.96	99.94	99.93	99.92	99.92	99.92	99.92

*1 — Biotite in cordierite.
2 — Edge of large biotite touching cordierite (UWG1E).
3 — Core of (2) away from cordierite.
4 — Biotite touching sillimanite and cordierite (UWG1H).
5 — Same grain and edge as (2), different location.
6 — Tiny biotite in cordierite, touching UCG1J.
7 — Edge of biotite touching cordierite (UCG1K).
8 — Small biotite in cordierite, touching UCG3B.
9 — Tabular biotite in cordierite, touching UCG3C and sillimanite inclusion.
10 — Small biotite in cordierite, touching UCG3F.
11 — Edge of large biotite touching cordierite (UCG5H).
12 — Large biotite in plagioclase.
**First two letters of title identifies laboratory (UW = University of
   Wisconsin, Madison, UC = University of California, Los Angeles, UA = The University of Arizona).

Table II.5. Sample CB7 — cordierites.

Sample* and Lab #**	1	2	3	4	5	6	7	8	9	10
	UWG2	UWG1E	UWG1F	UWG1H	UCG1J	UCG1K	UCG3B	UCG3C	UCG3F	UCG5H
SiO_2	50.96	50.74	50.63	50.97	47.99	47.75	47.95	48.24	48.05	47.99
Al_2O_3	32.92	32.23	32.72	32.41	32.57	32.58	32.40	32.46	32.14	31.67
TiO_2	.02	0.0	0.0	0.0						
FeO_t	9.96	10.20	10.22	9.68	10.30	10.04	9.87	10.16	10.27	9.33
MnO	.31	.24	.25	.24	.27	.26	.31	.27	.26	.28
MgO	6.51	7.37	7.22	7.76	7.28	7.34	7.29	7.23	7.28	7.30
CaO	.01	0.0	.01	0.0	.10	.07	.09	.11	.08	.11
Na_2O	.13	.08	.08	.13						
K_2O	.07	0.0	0.0	0.0						
H_2O										
Total	100.89	100.86	101.13	101.19	98.51	98.04	97.91	98.47	98.08	96.68

*1 — Cordierite near biotite.
2 — Cordierite touching biotite (UWG1C).
3 — Cordierite away from biotite.
4 — Cordierite touching biotite (UWG1G) and sillimanite.
5 — Cordierite touching biotite (UCG1W).
6 — Cordierite touching biotite (UCG1L).
7 — Cordierite touching biotite (UCG3A).
8 — Cordierite touching biotite (UCG3D).
9 — Cordierite touching biotite (UCG3E).
10 — Cordierite touching biotite (UCG5).
**First two letters of title identifies laboratory (UW = University of Wisconsin, Madison, UC = University of California, Los Angeles, UA = The University of Arizona).

Table II.6. Samples CB7 and CB5 — opaque oxide analyses.

Sample and Lab #*	UCG1W	UAG1F	UAG3Q
SiO_2	.11	.28	.33
Al_2O_3	.02	.07	.05
TiO_2	46.77	44.35	42.91
FeO_t	50.52	53.64	53.68
MnO			1.30
MgO	.19	.14	.29
Total	97.61	98.48	98.56

*First two letters of title identifies laboratory (UW = University of Wisconsin, Madison, UC = University of California, Los Angeles, UA = The University of Arizona).

Table II.7. Sample EC10a — analyses of garnet and biotite.

Sample* and Lab #**	1 UCG1A	2 UCG1B	3 UCG1P	4 UCG1O	5 UCG1L
SiO_2	35.45	34.73	35.62	35.61	38.06
Al_2O_3	24.13	21.38	22.39	22.14	21.96
TiO_2	1.48	2.50			
FeO_t	20.29	20.99	34.10	34.60	35.35
MnO	.13	.10	1.55	1.14	1.08
MgO	9.26	8.73	3.30	4.00	4.49
CaO	.02	.02	1.09	1.02	1.25
Na_2O	.15	.17			
K_2O	9.02	9.14			
H_2O	0.0	2.21			
Total	99.93	99.97	98.05	98.51	102.19

*1 — Biotite touching garnet rim.
 2 — Core of (1), above, away from garnet.
 3 — Garnet rim touching (1), above.
 4 — Garnet core, same grain as (3), above.
 5 — Garnet core, same grain as (3), above.
** First two letters of title identifies laboratory (UW = University
   of Wisconsin, Madison, UC = University of California, Los Angeles,
   UA = The University of Arizona).

LIST OF REFERENCES

Bence, A. E., and Albee, A. L., 1968, Empirical correction factors for
the electron microanalysis of silicates and oxides: Jour.
Geology, v. 76, p. 382-403.

Bryhni, I., and Griffin, W. L., 1971, Zoning in eclogite garnets from
Nordfjord, west Norway: Contr. Mineral. Petrol., v. 32,
p. 112-125.

Carmichael, D. M., 1969, On the mechanism of prograde metamorphic
reactions in quartz-bearing pelitic rocks: Contr. Mineral.
Petrol., v. 20, p. 244-267.

Chinner, G. A., 1960, Pelitic gneisses with varying ferrous/ferric
ratios from Glen. Cova, Angus, Scotland: J. Petrol., v. 1,
p. 178-217.

_____, 1962, Almandine in thermal aureoles: J. Petrol., v. 3, p. 316-
340.

Currie, K. L., 1971, The reaction 3 cordierite = 3 garnet + 4 sillimanite
+ 5 quartz as a geological thermometer in the Opinicon Lake
region, Ontario: Contr. Mineral. Petrol., v. 33, p. 215-226.

Edmunds, W. M., and Atherton, M. P., 1971, Polymetamorphic evolution of
garnet in the Fanad aureole, Donegal, Eire: Lithos, v. 4,
p. 147-161.

Evans, B. W., and Guidotti, C. V., 1966, The sillimanite-potash feld-
spar isograd in western Maine: Contr. Mineral. Petrol., v. 12,
p. 25-62.

Fisher, G. W., 1973, Non-equilibrium thermodynamics as a model for
diffusion-controlled metamorphic processes: Am. J. Sci., v. 273,
p. 897-924.

Fitton, J. G., 1972, The genetic significance of almandine-pyrope
phenocrysts in the calc-alkaline Borrowdale volcanic group,
northern England: Contr. Mineral. Petrol., v. 36, p. 231-248.

Gable, D. J., 1969, Geologic map of the Nederland Quadrangle, Boulder
and Gilpin Counties, Colorado: U. S. Geol. Surv. Quadrangle
Map GQ-833.

Gable, D. J., and Sims, P. K., 1969, Geology and regional metamorphism of some high-grade cordierite gneisses, Front Range, Colorado: Geol. Soc. Am. Spec. Paper, v. 128, p. 1-87.

Gable, D. J., Sims, P. K., and Weiblen, P. W., 1970, Thermal metamorphism of cordierite-garnet-biotite gneiss, Front Range, Colorado: J. of Geol., v. 78, p. 661-685.

Ganguly, J., 1972, Staurolite stability and related parageneses: theory, experiments, and applications: J. of Petrol., v. 13, p. 335-365.

Ganguly, J., and Kennedy, G. C., 1974, The energetics of natural garnet solid solution — I. Mixing of aluminosilicate end-members: Contr. Mineral. Petrol., v. 48, p. 137-148.

Grant, J. A., and Weiblen, P. W., 1971, Retrograde zoning in garnet near the second sillimanite isograd: Am. Jour. Sci., v. 270, p. 281-296.

Griffin, W. L., 1971a, Mineral reactions at a peridotite-gneiss contact, Jotunheimen, Norway: Mineral. Mag., v. 38, p. 435-445.

_____, 1971b, Genesis of coronas in anorthosites of the upper Jotun nappe, Indre Sogn, Norway: J. Petrol., v. 12, p. 219-243.

_____, 1972, Formation of eclogites and the coronas in anorthosites, Bergen arcs, Norway: Geol. Soc. America Mem., v. 135, p. 37-61.

Griffin, W. L., and Heier, K. S., 1973, Petrological implications of some corona structures: Lithos, v. 6, p. 315-335.

Griffin, W. L., and Råheim, A., 1973, Convergent metamorphism of eclogites and dolerites, Kristiansund area, Norway: Lithos, v. 6, p. 21-40.

Hall, A. J., 1941, The relation between color and chemical composition in the biotites: Amer. Min., v. 26, p. 29-33.

Harte, B., and Henley, K. J., 1966, Occurrence of compositionally zoned almanditic garnets in regionally metamorphosed rocks: Nature, v. 210, p. 689-692.

Heitanen, A., 1969, Distribution of Fe and Mg between garnet, staurolite, and biotite in aluminum-rich schist in various metamorphic zones north of the Idaho batholith: Am. Jour. Sci., v. 267, p. 422-456.

Helgeson, H. C., 1968, Evaluation of irreversible reactions in geo-
      chemical processes involving minerals and aqueous solutions --
      I. Thermodynamic relations: Geochim. Cosmochim. Acta, v. 32,
      p. 853-877.

Hollister, L. S., 1966, Garnet zoning: an interpretation based on the
      Rayleigh fractionation model: Science, v. 154, p. 1647-1651.

_____, 1969, Contact metamorphism in the Kwoiek area of British
      Columbia: An end-member of the metamorphic process: Bull.
      Geol. Soc. Am., v. 80, p. 2465-2494.

_____, 1970, Origin, mechanism, and consequences of compositional
      sector zoning in staurolite: Am. Mineral., v. 55, p. 742-766.

Hsu, L. C., 1968, Selected phase relationships in the system Al-Mn-
      Fe-Si-O; a model of garnet equilibria: J. Petrol., v. 9,
      p. 40-83.

Korzhinskii, D. S., 1959, Physiochemical Basis of the Analysis of the
      Paragenesis of Minerals, Consultants Bureau, New York.

Kurat, G., and Scharbert, H. G., 1972, Compositional zoning in garnets
      from granulite facies rocks of the Moldanubian zone, Bohemian
      massif of lower Austria, Austria: Earth Planet Sci. Letters,
      v. 16, p. 379-387.

Loomis, T. P., 1975, Reaction zoning of garnet: Contr. Mineral. Petrol.,
      v. 52, p. 285-305.

_____, 1976a, Irreversible reactions in high-grade metapelitic rocks:
      J. Petrol., in press.

_____, 1976b, Determining mass movements of metamorphic rocks from
      disequilibrium reactions: An example of the garnet granulite-
      gabbro transition: in Symposium on Geology and Petrology of
      the Crystalline Domains of the Earth's Crust, Proc. 25th
      International Geological Congress, Sydney, Australia.

Lovering, T. S., and Goddard, E. N., 1950, Geology and ore deposits of
      the Front Range, Colorado: U. S. Geol. Surv. Prof. Paper,
      v. 223, p. 1-319.

McAteer, C., 1976, Formation of garnets in a rock from Mallaig: Contr.
      Mineral. Petrol., v. 55, p. 293-301.

McLean, D., 1965, The science of metamorphism in metals: in Controls of
      Metamorphism, eds. W. S. Pitcher and G. W. Flinn, Edinburgh
      and London, Oliver and Boyd, p. 103-118.

Misch, P., and Onyeagocha, A. C., 1976, Symplectite breakdown of Ca-rich almandines in upper amphibolite-facies Skagit gneiss, north Cascades, Washington: Contr. Mineral. Petrol., v. 54, p. 189-224.

Mueller, R. F., 1967, Mobility of the elements in metamorphism: J. Geol., v. 75, p. 565-582.

_____, 1972, Stability of biotite: A discussion: Am. Mineral., v. 57, p. 300-316.

Okrusch, M., 1971, Garnet-cordierite-biotite equilibria in the Steinach aureole, Bavaria: Contr. Mineral. Petrol., v. 32, p. 1-23.

Perchuk, L. L., 1970, Equilibrium of biotite with garnet in metamorphic rocks: Geochem. Internat., v. 7, p. 157-179.

Råheim, A., 1975, Mineral zoning as a record of P, T history of Precambrian eclogites and schists in western Tasmania: Lithos, v. 8, p. 221-236.

Rast, N., 1965, Nucleation and growth of metamorphic minerals: in Controls of Metamorphism, eds. W. S. Pitcher and G. W. Flinn, Edinburgh and London, Oliver and Boyd, p. 73-102.

Sen, S. K., and Chakraborty, K. R., 1968, Magnesium-iron exchange equilibrium in garnet-biotite and metamorphic grade: Neues Jahrb. Mineral. Abh., v. 108, p. 181-207.

Shieh, Y. N., and Taylor, H. P., Jr., 1969, Oxygen and hydrogen isotope studies of contact metamorphism in the Santa Rosa Range, Nevada and other areas: Contr. Mineral. Petrol., v. 20, p. 306-356.

Smith, W. C., 1938, Geology of the Caribou stock in the Front Range, Colorado: Am. Jour. Sci., v. 36, p. 161-196.

Steiger, R. H., and Hart, S. R., 1967, The microcline-orthoclase transition within a contact aureole: Am. Mineral., v. 52, p. 87-116.

Thompson, J. B., 1959, Local equilibrium in metasomatic processes: in Researches in Geochemistry, ed. P. H. Abelson, New York, John Wiley, p. 427-455.

Tweto, O., and Sims, P. K., 1963, Precambrian ancestry of the Colorado mineral belt: Geol. Soc. America Bull., v. 74, p. 991-1014.

Vidale, R., 1969, Metasomatism in a chemical gradient and the formation of calc-silicate bands: Am. Jour. Sci., v. 267, p. 857-874.

Wones, D. R., and Eugster, H. P., 1965, Stability of biotite: experiment, theory, and application: Am. Mineral., v. 50, p. 1228-1272.

Wright, T. L., 1967, The microcline-orthoclase transformation in the contact aureole of the Eldora stock, Colorado: Am. Mineral., v. 52, p. 117-136.